



Review

# Synthesis and Characterization of Various Bimetallic Nanoparticles and Their Application

Nkosinathi Goodman Dlamini <sup>1</sup>, Albertus Kotze Basson <sup>1</sup> and Viswanadha Srirama Rajasekhara Pullabhotla <sup>2,\*</sup>

<sup>1</sup> Department of Biochemistry and Microbiology, University of Zululand, Private Bag X1001, KwaDlangezwa 3886, South Africa

<sup>2</sup> Department of Chemistry, University of Zululand, Private Bag X1001, KwaDlangezwa 3886, South Africa

\* Correspondence: pullabhotlav@unizulu.ac.za; Tel.: +27-35-902-6155

**Abstract:** Bimetallic nanoparticles are a complex nanoscale combination of two metal constituents. The superior properties of bimetallic nanoparticles (BNPs) compared with monometallic nanoparticles have attracted much attention from both scientific and technological perspectives. In recent years, many fabrication techniques have been proposed, and the detailed characterization of bimetallic nanoparticles has been made possible by the rapid advancement of nanomaterial analysis techniques. Metallic nanoparticles can be classified according to their origin, size, and structure, and their synthesis process can be physical, chemical, or biological. Bimetallic nanoparticles are more attractive than metal nanoparticles due to their unique mixing patterns and synergistic effects of two metal nanoparticles forming the bimetal. In this review, the different bimetallic synthesis methods and various characterization techniques are discussed. The paper will also discuss various applications for bimetallic nanoparticles. Different characterization techniques for bimetallic nanoparticles include X-ray diffraction (XRD) to investigate crystallinity and phase composition; the morphology and composition analysis of nanoparticles are studied using a scanning electron microscope fitted with an energy-dispersive X-ray analyzer (EDX); transmission electron microscopy (TEM), UV-vis spectrum, FTIR, and TGA analysis are also among the characterization tools used. Finally, we report on the various applications of BNPs, which include antimicrobial activity, pollutant removal, and wastewater application.

**Keywords:** application; bimetallic; synthesis



**Citation:** Dlamini, N.G.; Basson, A.K.; Pullabhotla, V.S.R. Synthesis and Characterization of Various Bimetallic Nanoparticles and Their Application. *Appl. Nano* **2023**, *4*, 1–24. <https://doi.org/10.3390/applnano4010001>

Academic Editor: Johann Michael Köhler

Received: 18 November 2022

Revised: 4 December 2022

Accepted: 21 December 2022

Published: 3 January 2023



**Copyright:** © 2023 by the authors. Licensee MDPI, Basel, Switzerland. This article is an open access article distributed under the terms and conditions of the Creative Commons Attribution (CC BY) license (<https://creativecommons.org/licenses/by/4.0/>).

## 1. Introduction

### 1.1. Bimetallic Nanoparticles as a Product of Nanotechnology

Bimetallic nanoparticles (BNPs) are a new type of nanomaterial made up of two different metal elements [1–3]. Although their synthesis is similar to that of their monometallic counterparts in some ways, the synergetic effect between the two components allows them to exhibit a wide range of new properties and applications [2]. BNPs have recently received a lot of attention from the research community due to their unique catalytic, electronic, optical, and magnetic properties [4]. Bimetallic nanoparticles are a type of material made up of two metals that exhibit new capabilities due to synergistic effects [5,6]. Bimetallic nanoparticles (nano alloys) have a higher application ability than monometallic nanoparticles. These nanoparticles can be classified as multi-shell, core-shell segregated, intermetallic (alloyed), or heterogeneous on the basis of the structural features resulting from the fabrication method [7,8]. Furthermore, synergistic effects, such as electron effect, lattice strain, bifunctional effect, and ensemble effect, significantly improve the specific physical and chemical properties of BMNPs [1]. The variety of these nanostructures is primarily determined by the nature of the combining metals, which is primarily determined by factors such as relative bond strength, surface energy, atomic dimensions, charge transfer, and specific electronic and magnetic effects [9].

Nanotechnology is crucial to many technological fields because of the constructed superstructures [10]. It saves energy and fuel by utilizing less material and renewable inputs whenever possible. Furthermore, nanotechnological products, processes, and applications are expected to significantly contribute to environmental and climate protection by conserving raw materials, energy, and water, as well as lowering greenhouse gas emissions and hazardous waste. Green nanotechnology's main advantages are increased energy efficiency, reduced waste and greenhouse gas emissions, and reduced consumption of non-renewable raw materials. Green nanotechnology provides an excellent opportunity to prevent negative consequences from occurring [11]. Atoms or molecules can be manipulated in this discipline to create structures with certain geometry and properties. It has uses in both the environment and human health, including effective medication administration [12,13] and solar energy harvesting [14,15], among others. Additionally, it contributes to a decrease in the usage of industrial chemicals, improving the environment's safety, security, and quality of life. In addition, it can be utilized for food packaging, cancer therapy, and water purification [6].

### 1.2. Nanoparticles of Various Types

All scientific phenomena that transpire in the dimension spanning the range of multiple atoms clusters, polymers, super molecular structure, and biomolecules is termed Nanoscience, i.e., it is the science of nanoscale and has the potential to revolutionize break-throughs in a range of fields across domains of all human activity [16]. Nanoscience has the ability to create a useful, safe, and healthy environment where hazardous pollutants and industrial chemicals can be removed through the use of more environmentally friendly nanotechnologies [17]. Development and synthesis of various nanomaterials is the emerging field of science referred to as Nanotechnology [18]. Objects with the size range between 1 and 100 nm are defined as nanoparticles and may differ from bulk material due to their size. To produce metallic nanoparticles, different metal salts are used as precursors; these metals include copper, iron, zinc, silver, gold, magnesium, titanium, and alginate [18]. To resolve problems/challenges such as renewable energies, effective drug delivery, human health, wastewater treatment, etc., diverse nanomaterials development needs to be extensively explored. Nanoscaled materials and nanoparticles encompasses novel and exceptional biological and physicochemical features [17,19,20].

Different types of nanoscale materials include, monometallic, bimetallic, trimetallic, or core-shell [6,21]. A combination of three different metals results in trimetallic nanoparticles and are considered more professional than bimetallic ones, while combination of two different metals results in a formation of bimetallic nanoparticles [21]. Monometallic nanoparticles synthesis involves the use of a single metal as a precursor. The trimetallic and bimetallic nanoparticles are receiving an enormous amount of attention, as opposed to monometallic, in both scientific and technological view; this is due to their catalytic properties that can be better tailored than those of monometallic nanoparticles [21]. Materials which have an inner structure and outer shell made of different components are termed core-shell nanoparticles [22,23]. Due to unique properties arising from the combination of core and shell materials, design, and geometry, these properties have gained interest from most researchers [24]. In addition, the biological properties possessed by these materials and antimicrobial activities of some bimetallic/core-shell nanoparticles, such as silver and copper, have attracted more interest from researchers [25,26].

In general, methods of nanoparticles synthesis can be divided into three groups: (1) chemical methods, (2) physical methods, and (3) bio-assisted methods [27]. The biological-assisted method is the method mostly preferred by researchers due to its environmental friendliness, as this method uses plant extracts or microorganism extract as the reducing and capping agent [28,29].

Metallic nanoparticles have been used in various fields as solutions to various problems faced by humans in recent years. The fields where nanoparticles are applicable include, electronics and IT applications, medical and healthcare applications, energy applications,

and environmental remediation [30]. Application of nanoparticles has contributed greatly to computing and electronics advances, leading to faster and more portable systems that can store and manage larger amounts of information [31]. Environmental problems, such as pollutant removal in water, acid mine drainage, dye removal in wastewater, and remediation have been addressed by the use of nanoparticles [32–35]. Medically, nanoparticles have been used as antimicrobial agents, in drug delivery, and in medical devices [25,36–38].

The synthesis of bimetallic nanoparticles—with uses in a variety of disciplines, including environmental remediation, wastewater treatment, and antibacterial action—is discussed in this review. This review emphasizes our own work and provides current advances in this area, which focuses on the production, characterization, and application of bimetallic nanoparticles in dispersion.

## 2. Synthesis Methods

### 2.1. Various Approaches to Bimetallic Nanoparticle Synthesis

For the preparation of supported bimetallic nanoparticles, a variety of synthesis techniques are available. This section summarizes some of the most common methods for bimetallic nanoparticles synthesis, as well as the potential benefits and drawbacks of each method. Researchers have discovered a variety of unique ways to manufacture nanoparticles that are of the proper size, content, and form, as these crucial attributes of nanoparticles have such a large impact on the material's qualities. Some of the methods for making nanoparticles are as follows:

#### 2.1.1. Thermal and Photochemical Decomposition

Precursors must be pyrolyzed at high temperatures in boiling solvents, but the main issue is that doing so makes it difficult to separate the reactive phase from the unstable nanocrystal phase. The majority of thermal procedures are endothermic because bond breakage requires a significant amount of energy. The photochemical method facilitates the isolation and study of nanomaterials with unusual size and composition [39,40].

#### 2.1.2. Electrochemical Reduction

In this process, electricity is used as the propellant or controller. Between two electrodes separated by an electrolyte, the electric current is carried [41]. For the purpose of creating metallic nanoparticles, the researchers used an electrochemical method [42]. The metallic anodic layer was removed, and the cathode transformed the metallic salt that was created into metallic particles. The generated metallic particles were stabilized by tetraalkylammonium salts. Electrochemical technique has several benefits, including affordability, high particle purity, the ability to change particle size by varying current density, and ease of use. The majority of industrial settings use this strategy.

#### 2.1.3. Chemical Reduction

With this method, zero-valent metal nanoparticles are produced. This strategy uses two mechanisms: reduction and the interaction of metallic and polymeric substances. Other reducing agents used include sodium borohydride, elemental hydrogen, Tollen's reagent, and ascorbate. Chemical reduction is a common process in the production of nanoparticles [43]. In addition, copper nanoparticles have been synthesized by chemical reduction [44].

The most promising methodology or method for producing core-shell structured bimetallic nanoparticles is through sequential reduction [45]. It involves the deposition of a metal on monometallic nanoparticles made of another metal. The resynthesized monometallic nanoparticles must be chemically surrounded by the deposited metal atom [46].

#### 2.1.4. Sputtering

Sputtering is a procedure in which high-energy external stimuli are used to dislodge nanoparticles from the surface of a target material [47]. Nanoparticles are ejected only when the quantity of energy delivered is greater than that provided by ordinary thermal

energies. This approach yields high-purity nanoparticles. Magnetic sputtering, for example, is used to make silicon nanowires. This approach has some disadvantages, such as a lack of control over particle form and a significant energy consumption for electron ejection. Because a high temperature is necessary, it might be dangerous, resulting in a variety of skin problems.

#### 2.1.5. Sol–Gel Method

Sol and gel are the two words that make up the sol–gel method [48]. Sol is a stable colloidal solid particle dispersion in liquid. Only Vander-Waal forces are present in sol because the scattered phase is so small. The concentration of the solid in a gel is greater than that of the liquid. The particles or ions that are still present after evaporation form a continuous network within the semi-rigid bulk. Most gel systems contain coulombic interactions. These two network functions are mixed together in the sol–gel method. The two main stages in this method are hydrolysis and condensation. Several BNPs, including Au-Ag, Au-Pd, and Au-Pt, are made using the sol–gel method [49–51]. This technology is beneficial because it is a straightforward, cost-effective, and efficient way to generate high-quality nanoparticles [52]. It is intriguing because it is a low-temperature technology that allows for the management of the chemical composition of product.

#### 2.1.6. Chemical Precipitation Method

In chemical precipitation, a liquid is converted into a solid by making the liquid into an insoluble form or by causing the solution to be supersaturated. Chemical reagents are added to the solution and the precipitates are then separated from it [6,46,52,53]. It is a very important approach since it is a single-step procedure that aids in the large-scale manufacture of nanoparticles without any contaminants. It also aids in water purification and is a long-term solution that yields permanent results.

### 2.2. Synthesis of Bimetallic/Nanoparticles Using a Bioflocculant

Monometallic nanoparticles were synthesized using bacterial extract (bioflocculant) as a reducing agent. First, 50 mL distilled water was used to prepare 0.003 M solution of iron sulphate. This solution was followed by addition of 0.5 g of purified bioflocculant extracted from *Alcaligenes faecalis* which was previously isolated from a marine environment [54]. The mixture was agitated in an incubator for 5–10 min at room temperature before being permitted to stand for 24 h (Figure 1). The precipitate was collected using a centrifuge at 4 °C, 8000 rpm for 15 min. It was then cleaned with 100% pure ethanol to get rid of any contaminants and then vacuum-dried. The physical observation and characterization of iron nanoparticles (FeNPs) proved their synthesis. Bimetallic nanoparticles (Fe/Cu BNPs) were created by mixing produced FeNPs in various amounts, 10, 20, and 30 mL (1 mg/mL), with a stabilizing solution of CuSO<sub>4</sub> (0.003 M) in 6.0 mL of 5.0 M glucose. The reaction was allowed to continue for 20 min, and the formed precipitate was collected using centrifuge at 15,000 rpm for 30 min at 4 °C.

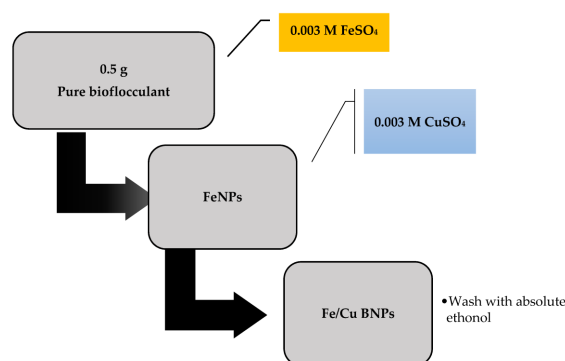


**Figure 1.** Schematic of the Fe/Cu BNPs synthesis process.

### 2.3. Nanoparticles Characterization

#### 2.3.1. Nanoparticles X-ray Diffraction (XRD)

To investigate crystallinity and phase composition of the metallic nanoparticles, Bruker Advance D8 diffractometer equipped with Cu-K $\alpha$  radiation ( $\lambda = 1.5406 \text{ \AA}$ ) operated at 40 kV, 40 mA at room temperature was used. A sample holder was used to place dry samples, and diffraction patterns were recorded in the  $2\theta$  range from  $10^\circ$  to  $80^\circ$  at scanning speed of  $0.5^\circ/\text{min}$  [55].

#### 2.3.2. Morphology and Elemental Analysis of Nanoparticles (SEM-EDX)

The morphology and composition analysis of nanoparticles were studied using a scanning electron microscope (JEOL JSM-6100) fitted with an energy-dispersive X-ray analyser (EDX). SEM pictures were captured using a tungsten (W) filament that was operated at an emission current accelerator voltage of 100 A and 10 kV. A small amount of the material was deposited on double-sided carbon tape on a copper stub and coated with carbon to prepare an SEM sample [56].

#### 2.3.3. Transmission Electron Microscope (TEM) Analysis

Following Kaasalainen, et al. [57], the nanoparticles were photographed using a TEM with a JEOL 1010 transmission electron microscope. Samples were prepared by applying a diluted suspension in toluene to a copper grid (150 mesh) using a micropipette. Samples were then left to dry at room temperature. Samples were viewed at an accelerating voltage of 100 kV. Images were captured using a Megaview III camera and recorded and quantified using Soft Imaging System iTEM software.

#### 2.3.4. Fourier Transform–Infrared (FT-IR) Analysis of Nanoparticles

Fourier Transform–Infrared (FT-IR) spectroscopy (Tensor, Bruker) was used to confirm functional groups present in the nanoparticles [58]. The FT-IR spectra were recorded for the dry powder samples with a resolution of  $4 \text{ cm}^{-1}$  in the range of  $4000\text{--}200 \text{ cm}^{-1}$ .

#### 2.3.5. Thermogravimetric Decomposition Analysis of Nanoparticles (TGA)

Perkin-Elmer Thermal Analysis Pyris 6 TGA was used for thermostability analysis of the nanoparticles [59]. The samples were heated in a temperature range between  $22$  to  $900 \text{ }^\circ\text{C}$  under constant nitrogen gas flow at a constant rate of ramping,  $10 \text{ }^\circ\text{C min}^{-1}$ .

#### 2.3.6. UV–Vis Analysis of Nanoparticles

To investigate the absorption of nanoparticles Perkin-Elmer UV–visible spectrophotometer was used, Begum, et al. [60]. The amount of 2 mL of deionized water was used to dilute 0.1 mL of the samples. The investigation was conducted in the wavelength region of 300 to 700 nm operated at a resolution of 1 nm as a function of time.

#### 2.3.7. Flocculation Activity Analysis of Nanoparticles

Kaolin clay was utilized as a test material to measure the flocculation activity of bimetallic nanoparticles using a slightly modified approach, as described by Kurane, et al. [61]. Here, 100 mL of a kaolin solution was combined with 2 mL of bimetallic nanoparticles (0.2 mg/mL) and 3 mL of  $\text{CaCl}_2$  (1 g/L) in a 250 mL conical flask to create a suspension of 4 g/L of kaolin solution. The mixture was stirred at 165 rpm for one minute before being poured into a graduated measuring cylinder with a capacity of 100 mL and allowed to stand for five minutes. After that, a Pharo 100 Spectrophotometer<sup>®</sup> was used to analyze the flocculation activity in the upper portion of the flocculated kaolin solution (Capital Lab Supplies CC, Durban, South Africa). To calculate flocculation activity, the following equation was used:

$$\text{Flocculation activity (FA)\%} = (A - B)/A \times 100$$

where A is the optical density of the control at 550 nm, and B is the optical density of the sample at 550 nm.

### 2.3.8. Evaluation of Bimetallic Nanoparticles for Wastewater Treatment and Dye Removal

To evaluate the ability of bimetallic nanoparticles to remove pollutants in wastewater, a method by Dlamini, Basson, Shandu, Mavuso and Pullabhotla [32] was followed. Briefly, pollutants such as BOD, COD, sulphur, nitrite, etc., were used to evaluate the effectiveness of bimetallic nanoparticles, while dyes such as methyl orange, safranin, malachite green, and methylene blue were used to evaluate dye removal potential by nanoparticles. Removal efficiency (RE) was calculated using the following equation:

$$\text{Removal efficiency (RE)\%} = (C_i - C_f)/C_i \times 100$$

where  $C_i$  is the starting value prior to the inclusion of nanoparticles, and  $C_f$  is the value following the nanoparticle treatment.

## 2.4. Antimicrobial Activity Evaluation of Bimetallic Nanoparticles

### 2.4.1. Minimal Inhibitory Concentration (MIC)

Antimicrobial activity determination of bimetallic nanoparticles was achieved through the use of 96 micro-well plates, as described by Eloff [62]. The lowest concentration required to inhibit growth of microorganism is described as MIC [3]. The amount of 50  $\mu\text{L}$  of sterile nutrient broth was inoculated in all wells of 96-well plates, followed by 50  $\mu\text{L}$  of 0.2 g of bimetallic nanoparticles dissolved in 2 mL of distilled water. The bimetallic solution (50  $\mu\text{L}$ ) was poured only into the first row of 96-well plates containing 50  $\mu\text{L}$  sterile nutrient broth and mixed. A 3-fold dilution method was adopted whereby (50  $\mu\text{L}$ ) from row A was taken to row B of the 96 micro-well plates and was mixed again. Taken from row B (50  $\mu\text{L}$ ), the bimetallic nanoparticles were mixed with the successive rows until they were present in varying concentrations across the entire well. Test strains were then added (50  $\mu\text{L}$ ) into the matching micro-wells, which had a total volume of 50  $\mu\text{L}$ . Ciprofloxacin (40%) was employed as an affirmative control, and distilled water as a negative control. Plates were incubated overnight at 37  $^{\circ}\text{C}$  with the addition of test microorganisms, and P-iodonitrotetrazolium violet (INT) solution was employed as an indicator. Each well received 40  $\mu\text{L}$  of 0.2 mg/mL INT solution, which was then added and incubated for an additional 30 min at 37  $^{\circ}\text{C}$ .

### 2.4.2. Minimal Bactericidal Concentration (MBC)

Agar dilution method was used to determine MBC. For wells that did not indicate colour change, a loop full of culture of each strain from the well was streaked on a Mueller Hilton nutrient agar and incubated for 12 h at 37  $^{\circ}\text{C}$ . The lowest concentration of bimetallic nanoparticles that exhibited the complete killing of the test organisms were considered as the MBC [63–65].

## 2.5. Mechanisms for BNPs' Formation and Factors Affecting Their Synthesis

Pan, et al. [66] stated that a detailed understanding of the particle's formation mechanism is required for success in either particle design or scale-up and will greatly benefit the development of structure-controlled synthesis pathways for bimetallic nanoparticles. Furthermore, the availability of high-intensity tunable X-ray sources at synchrotron facilities worldwide has made X-ray absorption spectroscopy (XAS) a powerful tool for studying the nucleation and growth (mechanism of BNPs formation) processes during nanoparticle formation. Temperature, pH, reaction time, and metal ion concentration are all factors that influence BNP biosynthesis. Chemical and physical factors influence the size and shape of the NPs [67,68].

### 3. Results

#### 3.1. Synthesis of Bimetallic Nanoparticles by Different Biological Techniques

Table 1 below shows some nanoparticles synthesized using various methods and reducing agents.

**Table 1.** Bimetallic nanoparticles synthesized by different methods.

Synthetic Technique	Type of Reducing Agent	Type of Bimetallic Nanoparticles	Reference
Biological	Biofloculant	Fe/Cu	[69]
Chemical		Pd/Pt	[70]
Biological	Plant extract	Ti/Ni	[71]
Biological	Starch	Fe/Pd	[72]
Physical/chemical		Pt/X (X = Cu, Au, or Ag, etc.)	[6]
Physical/chemical		Pd/Fe, Pd/Zn, Pt/Fe, Ni/Fe	[6]
Biological	Microorganism	Au/Ag	[73]
Biological	Red alga, <i>Gracilaria</i> sp. <i>Oscimum basilicum</i>	Ag/Au	[74]
Biological	(Basil) flower, and leaf extracts	Au/Ag	[75]
Physical		Ag/Cu	[76]
Biological	Peptides	Au/Pd	[77]
Chemical		Fe/Ni	[78]
Chemical		Cu/nZVI	[79]
Chemical		Cu/Ni	[80]
		Fe/Cu	[81]
Biological	<i>Phoenix dactylifera</i> leaves	Cu/Ag	[82]

#### 3.2. Characterization of Bimetallic Nanoparticles

##### 3.2.1. X-ray Diffraction Studies

The XRD analysis was conducted on Fe/Cu bimetallic nanoparticles to study the nature of interaction between the two metal precursors and the biofloculant. From Figure 2, different diffraction patterns were observed at  $2\theta \sim 10\text{--}80^\circ$ .

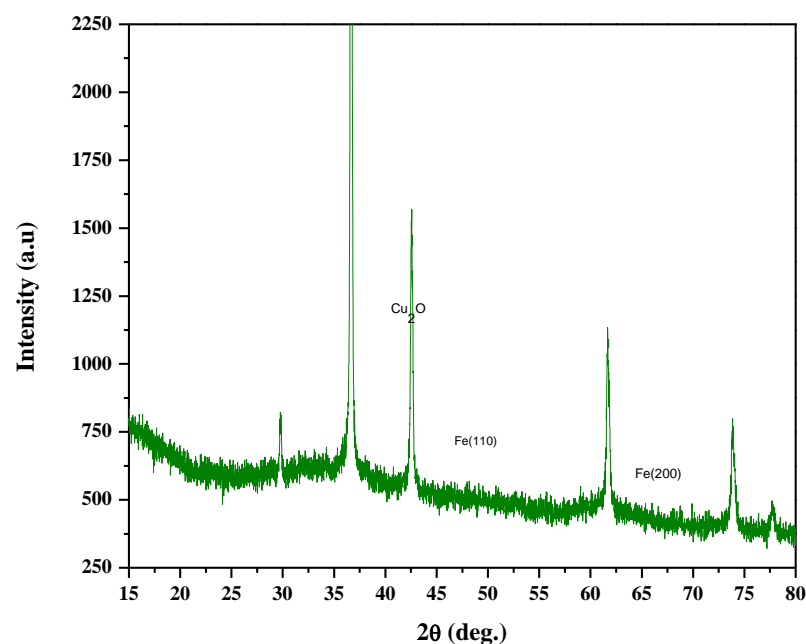


**Figure 2.** X-ray diffraction patterns of Fe/Cu bimetallic nanoparticles. Adopted from [83].

### 3.2.2. FT-IR Analysis of Fe/Cu Bimetallic Nanoparticles

The FT-IR spectrum of Fe/Cu is shown in Figure 3. The IR spectrum showed the presence of functional groups, such as hydroxyl and amine.

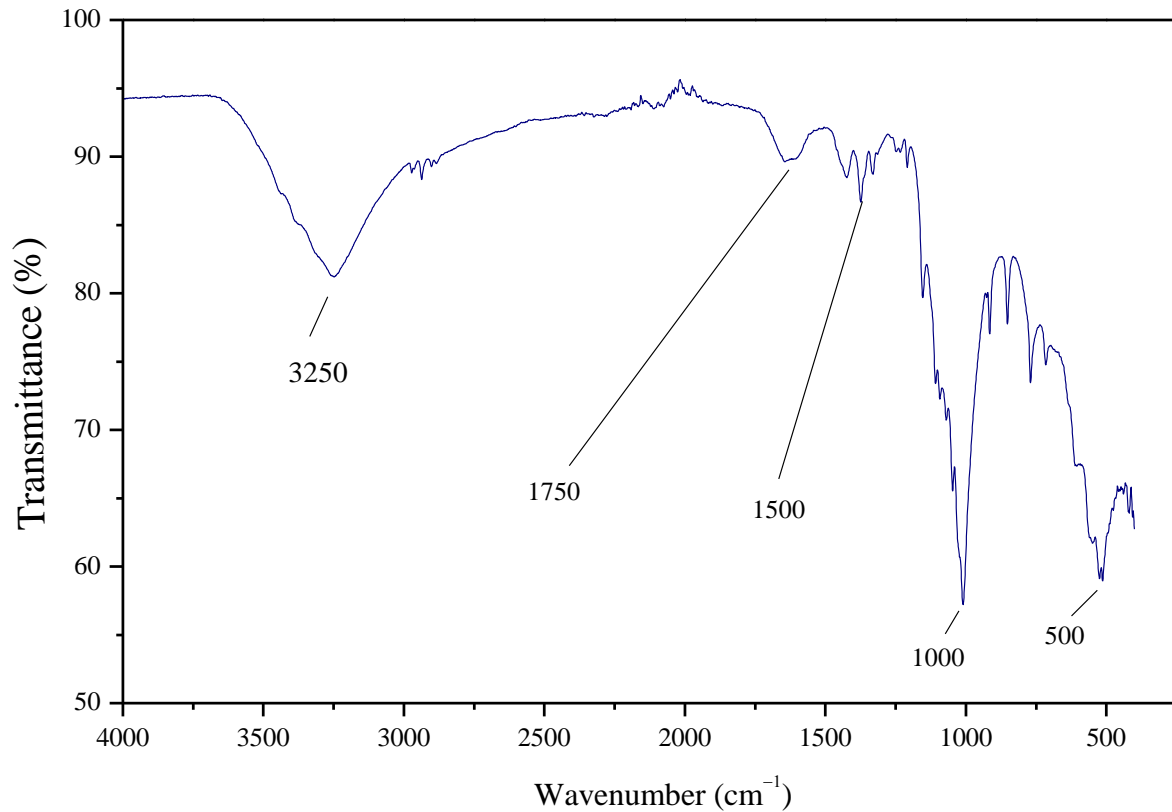


**Figure 3.** FT-IR analysis of Fe/Cu bimetallic nanoparticles.

### 3.2.3. SEM Analysis of Fe/Cu Bimetallic Nanoparticles

The morphological and elemental analyses of biofloculant and Fe/Cu nanoparticles is shown below in Table 2 and Figures 4 and 5, respectively.

**Table 2.** Elemental composition of the biofloculant and nanoparticles.

Elements	Sample	
	Biofloculant (wt.%)	Fe/Cu BNPs (wt.%)
C	13.21	19.07
O	55.25	55.09
Mg	13.35	12.27
P	16.00	0.63
K	0.14	0.24
Ca	2.04	0.7
Fe	-	1.19
Cu	-	3.83
Na	-	7.01
Cl	-	0.20
<b>Total</b>	<b>100.00</b>	<b>100.00</b>

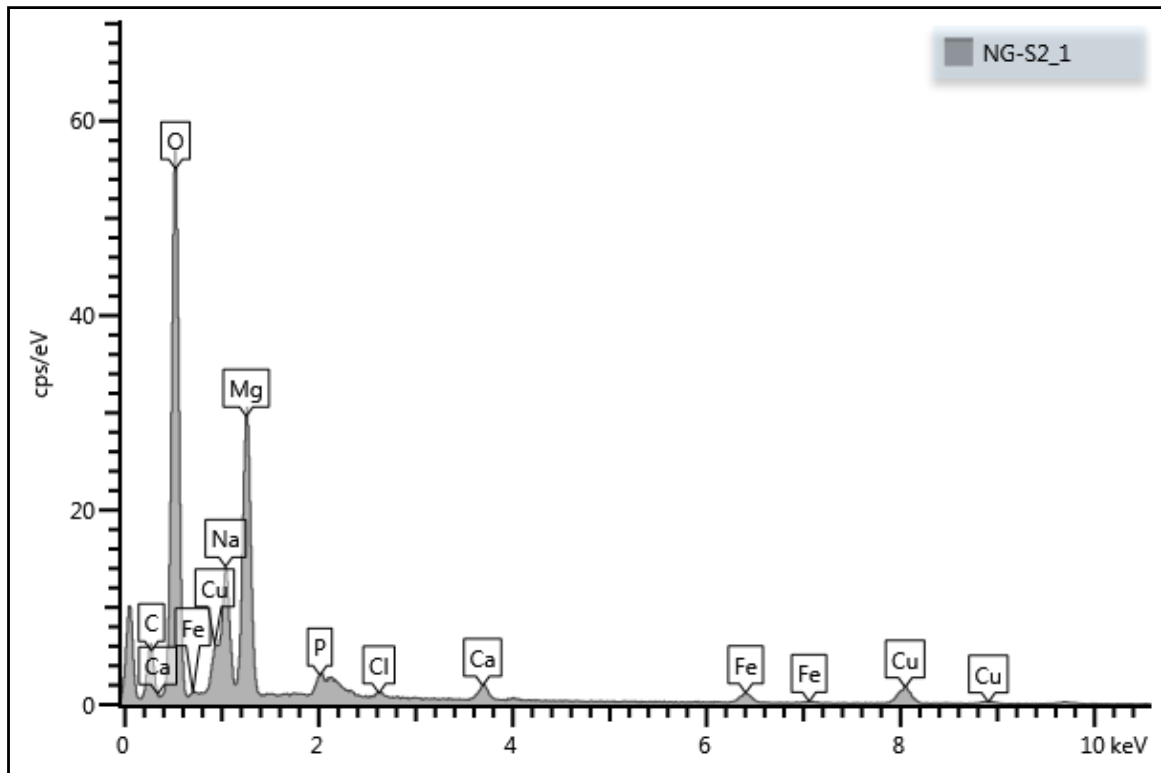


Figure 4. SEM-EDX analysis of Fe/Cu bimetallic nanoparticles.

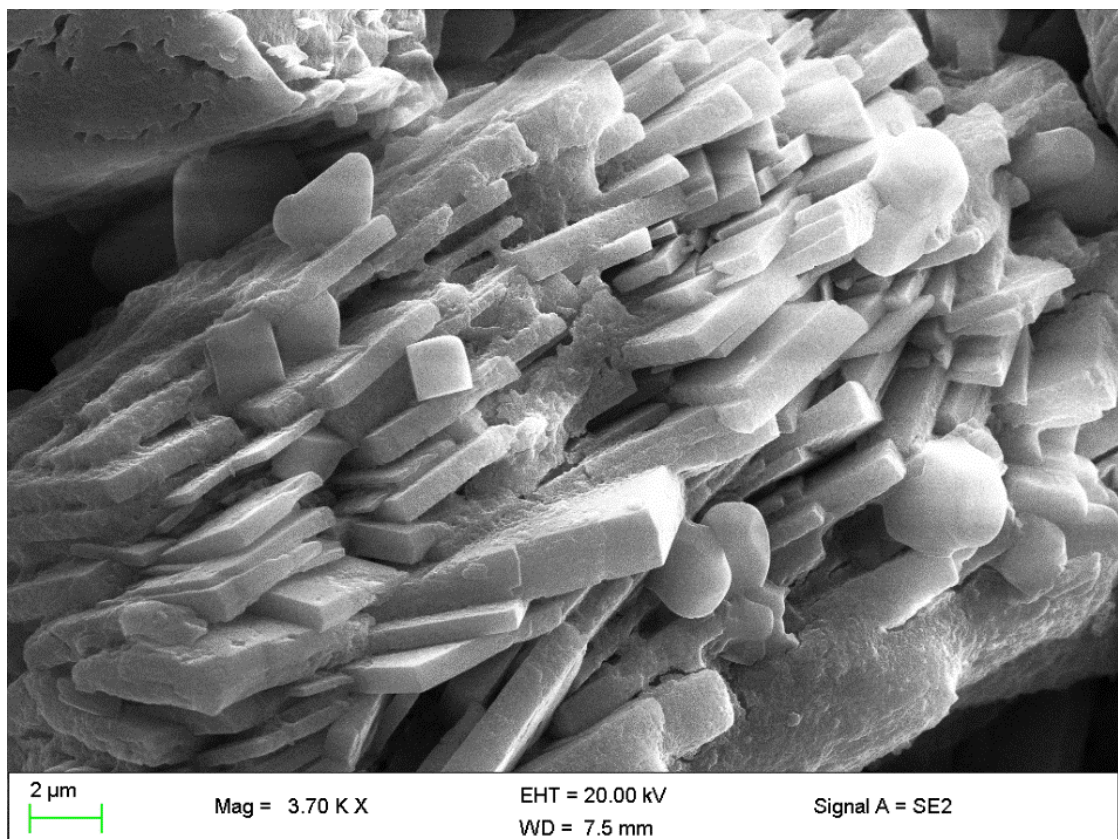
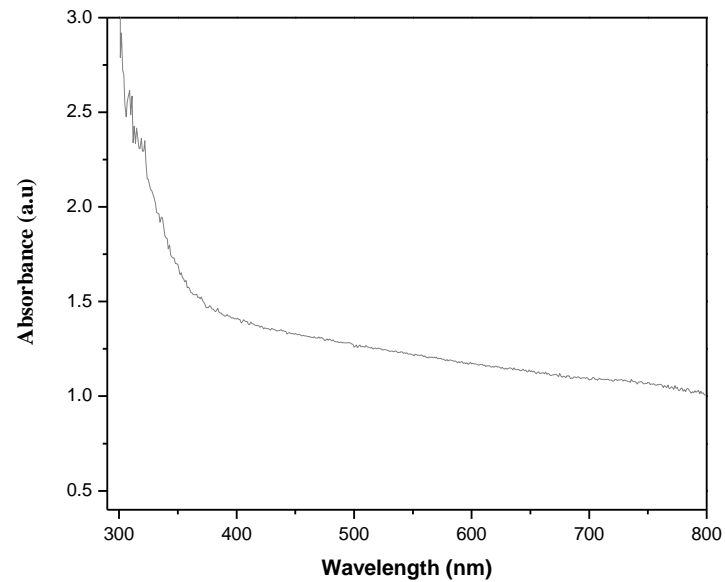


Figure 5. SEM image of Fe/Cu bimetallic nanoparticles.

### 3.3. UV–Vis Analysis of Fe/Cu Bimetallic Nanoparticles

Figure 6 below represents the results obtained from the analysis of Fe/Cu nanoparticles by UV–vis spectrophotometer.



**Figure 6.** UV–vis analysis of Fe/Cu bimetallic nanoparticles.

### 3.4. TEM Analysis of Fe/Cu Bimetallic Nanoparticles

Figure 7 represents the TEM image of Fe/Cu bimetallic nanoparticles.

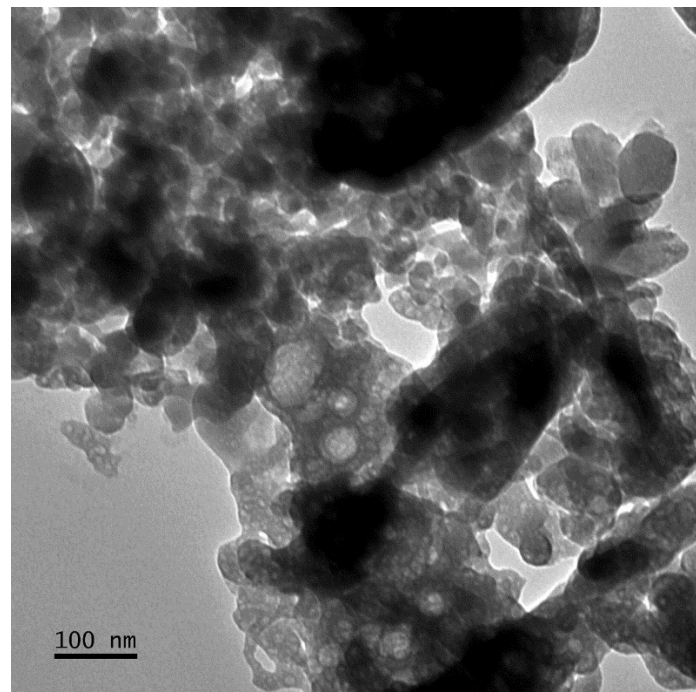


**Figure 7.** TEM analysis of Fe/Cu bimetallic nanoparticles.

### 3.5. Application of Fe/Cu Bimetallic Nanoparticles in Flocculation

Table 3 shows the effects of various parameters on flocculation activity. The nanoparticles were shown to be cation-independent and effective at low concentrations.

**Table 3.** Effect of different parameters on flocculation activity (FA) of bimetallic nanoparticles.

Flocculant		Parameters						
Fe/Cu	Dosage (mg/mL)	FA (%)	Cations	FA (%)	Temperature (°C)	FA (%)	pH	FA (%)
	0.2	99 <sup>a</sup>	Na <sup>+</sup>	97 <sup>a</sup>	27	99 <sup>a</sup>	3	95 <sup>a</sup>
	0.4	98 <sup>a</sup>	Ca <sup>2+</sup>	99 <sup>a</sup>	60	93 <sup>a</sup>	7	99 <sup>a</sup>
	0.6	98 <sup>a</sup>	Fe <sup>3+</sup>	97 <sup>a</sup>	80	97 <sup>a</sup>	11	95 <sup>a</sup>
	0.8	93 <sup>b</sup>	Control	95 <sup>a</sup>	100	96 <sup>a</sup>		

Percentage flocculating activity with different letters (<sup>a</sup> and <sup>b</sup>) are significantly ( $p < 0.05$ ).

### 3.6. Antimicrobial Activity of Bimetallic Nanoparticles

The antibacterial activity of several nanoparticles is presented in the Table 4 below. Several nanoparticles in the environment have been discovered to be efficient against bacteria.

**Table 4.** Antibacterial activities of different bimetallic nanoparticles.

Type of Nanoparticles	Name of Microorganisms	Antimicrobial Activity	Reference
Fe/Cu	<i>Escherichia coli</i>	+ve	[84]
	<i>Bacillus pumilus</i>	+ve	
	<i>A. freundii</i>	+ve	
	<i>Klebsiella pneumoniae</i>	+ve	
Au/Pt	<i>Escherichia coli</i>	+ve	[85]
	<i>Klebsiella pneumoniae</i>	+ve	
	<i>Salmonella choleraesius</i>	+ve	
	<i>Pseudomonas aeruginosa</i>	+ve	
Ag/Au	<i>Salmonella typhi</i> and <i>Escherichia coli</i>	+ve	[74]
	<i>Klebsiella pneumoniae</i>	+ve	
	<i>Staphylococcus aureus</i>	+ve	
	<i>Pseudomonas aeruginosa</i> ,	+ve	
Au/ag	<i>Staphylococcus aureus</i>	+ve	[75]
	<i>Bacillus subtilis</i>	+ve	
Ag/Cu	<i>Escherichia coli</i>	+ve	[76]
	<i>Bacillus subtilis</i>	+ve	
Cu/Ag	<i>Bacillus subtilis</i>	+ve	[82]
	<i>Escherichia coli</i>	+ve	

### 3.7. Comparison of Physical, Chemical, and Biological Methods for Producing Bimetallic Nanoparticles

The comparison of different methods of nanoparticle synthesis is shown in Table 5 below. The biological method is proposed as the most suitable compared to the chemical and physical methods available in literature.

**Table 5.** Comparison of different techniques for bimetallic synthesis.

Method Type	Advantage	Disadvantage
Chemical	Less complicated, less expensive, can synthesize diverse sizes and shapes, large quantities can be obtained in a short period of time, and doping of foreign atoms during synthesis is possible [86].	Chemicals used as reducing agents may have negative effects as hazardous byproducts [87].

Table 5. Cont.

Method Type	Advantage	Disadvantage
Biological	Mazhar, Shrivastava and Tomar [86] found that the processes are environmentally friendly, take less time, produce almost no industrial waste, and do not use toxic chemicals.	
Physical	These methods have some advantages over chemical methods, such as no solvent contamination in the prepared film and uniformity in the formation of nanoparticles [86].	These methods necessitate the purchase of expensive equipment, and the final yield is low [87].

#### 4. Discussion

Different bimetallic nanoparticles were synthesized using different approaches, as indicated in Table 1. Biological techniques, with plant extract, microorganism extract (biofloculant), starch, and microorganism, have been used [69,71–73]. Physical and chemical techniques have been also used to obtain zero-valent bimetallic nanoparticles in the past [88]. This includes nanoscale zero-valent copper iron particles (Cu/nZVI). For reducing chemical consumption, physical methods are preferred for bimetallic nanoparticles synthesis, but it requires extremely high energy to maintain. On the contrary, due to the high-yield–low-cost technologies and growth controlling options, chemical methods are most commonly used. However, their application is limited due to the use of solvents and chemicals, which renders them environmentally unfriendly. On the other hand, biological methods can overcome both shortcomings of the chemical and physical methods for synthesis of bimetallic nanoparticles. Nevertheless, resultant particle aggregation tendency and the least provision for growth controllability are the constraining factors [89]. Ionic salt is reduced in a suitable medium in the presence of surfactants using various reducing agents in the chemical reduction process [90]. To generate metal nanoparticles, a reducing agent, such as sodium borohydride, is utilized in an aqueous solution. While chemical reduction is the easiest way to prepare metal nanoparticles, there are various disadvantages to reducing agents, including toxicity, expense, poor reducing ability, high cost, and impurities [91]. The use of naturally occurring resources, such as microorganisms, for the manufacture of nanoparticles is becoming increasingly popular around the world. Because of their abundance in the environment and capacity to adapt to severe conditions, prokaryotes have received attention as a source of metallic nanoparticle production. Bacteria have a number of benefits, including rapid reproduction and ease of cultivation and manipulation [92]. Controlling variables, such as oxygenation, temperature, and incubation period, can help to control growth. Changing the pH of the growth media during incubation produces nanoparticles of various sizes and shapes [93]. For the formation of metallic nanoparticles, such as gold, silver, copper, and zinc, a range of plant products, such as extracts, are used. Plant secondary metabolites, such as phenolic acid, flavonoids, terpenoids, and alkaloids, are abundant in the crude extracts, which preferentially decrease metallic ions and lead to the creation of bulk metallic nanoparticles. Plant metabolites, both primary and secondary, are regularly involved in redox reactions in plant metabolic pathways. These qualities are used as a reducing and capping agent, resulting in the production of environmentally friendly nanoparticles [94]. The disadvantage of this approach is that it necessitates heating conditions, such as temperature, which raises the cost of nanoparticle production. Plant extracts, unlike other pathogenic microbes, do not have the same pathogenicity as fungi and bacteria. Nanoparticles that are fairly homogeneous are created [92].

Table 5 represents different approaches for BMNPs synthesis and their advantages and disadvantages. Physical methods have some advantages over chemical methods, such as no solvent contamination in the produced film and uniformity in nanoparticle formation. Several physical methods of nanoparticle synthesis can be used, including

laser irradiation methods: bimetallic nanoparticles can be synthesized without using any chemical agents and only by high-intensity laser irradiation on an aqueous solution [86]. Chemical methods: the advantages over physical methods are that the techniques are uncomplicated, economical, different sizes and shapes can be synthesized, large quantities can be obtained in a short time, and doping of foreign atoms during synthesis is possible. One of the different chemical synthesis methods is the inverse micelle method: inverse micelles are found in water-in-oil microemulsions of specific composition in the form of nanometric-sized droplets. Biological methods: Several advantages of biological methods over chemical and physical methods are that the processes are environmentally friendly, take less time, generate almost negligible industrial waste, do not use toxic chemicals, use methods with biological properties to produce nanoparticles, are safe, and have diverse applications that are not possible with physical or chemical synthesis methods [95]. The physical and chemical synthesis of nanoparticles is costly, dangerous, and time-consuming. As a result, more emphasis is being placed on the “green synthesis” of nanoparticles using natural resources, such as plants and microbes [96,97]. Plant synthesis of nanoparticles is superior to microbe synthesis because it does not require synthesis protocols or toxic chemicals and has a higher reaction rate because microbes do not need to be cultured.

Commercial polysaccharides are not cost-effective, but they are emerging as stabilizing and reducing agents for the synthesis of nanoparticles. Exopolysaccharides made by microorganisms, such as biofloculants, therefore, present a promising alternative for nanoparticle production and stability [84,98]. Fe/Cu bimetallic nanoparticles' X-ray diffraction patterns are displayed in Figure 2. The broad peak at  $2\theta$ ,  $45^\circ$  indicates the presence of an iron amorphous phase.  $\text{Cu}_2\text{O}$  and iron oxide (FeO) crystalline phases are present, as indicated by apparent peaks at the  $2\theta$  of  $34.9^\circ$  and  $45.8^\circ$  [99,100]. On the contrary, Shao, et al. [101] reported the diffraction peaks with  $2\theta = 43.4^\circ$  and  $50.4^\circ$ , which corresponded to copper. The smaller particle size is generally indicated by the wider peaks. When compared with pure Cu and Fe, the diffraction peaks exhibit minimal change, demonstrating that the Cu atoms have replaced the Fe atoms [102]. Similarly, Younas, et al. [103] also alluded that the presence of minor peaks indicates the presence of impurity in the form of biomolecules. The presence of Fe/Cu nanoparticles and their crystalline nature was confirmed by the sharp and intense peaks.

FT-IR characterisation was carried out to investigate potential binding sites for the biofloculant's stabilization of Fe/Cu. The bands on the infrared spectrum provide information about many chemicals surrounding Fe/Cu nanoparticles, including amides, alcohols, proteins, etc. [104]. The molecular structures and chemical bonding that significantly contribute to the production of nanoparticles are displayed in the FT-IR spectrum of synthetic Fe/Cu bimetallic nanoparticles (Figure 3). According to Mata, et al. [105], the presence of the OH group is crucial for stabilizing the production of nanoparticles. The hydroxyl (OH) and amine ( $\text{NH}_2$ ) groups can be distinguished by the strong band at  $3250\text{ cm}^{-1}$ . Asymmetrical stretching peak at  $1743\text{ cm}^{-1}$  and symmetrical medium stretching peak at  $1380\text{ cm}^{-1}$  both demonstrated the presence of the carboxyl group (COH), while a peak at  $1022\text{ cm}^{-1}$  indicates the presence of a methoxyl group, which is seen by stretching the C-O, and peaks at  $734\text{--}513\text{ cm}^{-1}$  indicate the existence of saccharide derivatives. Wang's study used a post-impregnation and sodium borohydride reduction strategy to create bimetallic nanoparticles. The results revealed the characteristic bands at  $796$  and  $1060\text{ cm}^{-1}$ , which correspond to symmetric and anti-symmetric Si-O stretching, respectively. The bending and stretching vibration of -OH, which results from the dissociative chemisorption of water molecules, is responsible for the absorption band centering at  $1630\text{ cm}^{-1}$  and the broad band between  $2900$  and  $3700\text{ cm}^{-1}$  observed for all samples [106]. The surface of colloidal particles has  $\text{H}^+$  and  $\text{OH}^-$  groups, which may interact with the nanoparticle chains to produce hydrogen bonds that allow for bigger floc production. The functional groups also help in the flocculation process [83].

SEM micrographs of Fe/Cu were obtained in order to get more direct information about the morphology of prepared bimetallic nanoparticles, as shown in Figure 5. The

SEM image (Figure 5) of the nanoparticles showed an irregular shape, and nanoparticles seemed to be agglomerated [101]; due to the magnetic forces and high surface tension, the growth and crystallization of Fe/Cu are under the control [107]. In another study by Younas et al. [103], where Fe-Cu nanoparticles were synthesized, information was provided on the morphology of the nanoparticles, which appeared to have a heterogeneous surface. The micrographs show a mixture of cubic and rectangular nanoparticle morphologies. Furthermore, nanoparticle SEM images show a spherical morphology with a smooth surface and a uniform diameter of approximately 560 nm in a study reported by Wang, Liu, Hussain, Li, Li, Sun, Shen, Han and Wang [106].

Table 2 shows the results of elemental composition of the biofloculant and nanoparticles. The existence of numerous elements, such as C, O, Mg, P, K, Ca, Fe, Cu, Na, and Cl, was revealed by SEM-EDX analysis. Cu and Fe were not found in the biofloculant sample; however, Cu and Fe were found in 3.83 wt.% and 1.19 wt.%, respectively, in the nanoparticle sample. The presence of the other elements indicates that the biofloculant is polysaccharide in nature [108]. Furthermore, components, such as Na, P, and K, are derived from the growth media used to produce biofloculant.

The Cu/Fe UV-Visible spectrum was obtained between 350 and 800 nm since copper nanoparticles are often known to exhibit surface plasmon response (SPR) bands within that specific range [104]. The shape and size of the particles, as well as the type of solvent employed in the synthesis, affect the SPR peaks; the smaller the nanoparticle size, the more an SPR band's bandwidth increases. The absorption peak of the produced nanoparticles revealed a shift in wavelength to a smaller wavelength at approximately 320 nm (Figure 6). The bimetallic nanoparticles' inclusion of both Fe and Cu may be responsible for this. BNPs formation is influenced by different factors, such as pH, temperature, metal ion concentration, and reaction time [67]. The pH value is an important experimental parameter in the dynamics of NP growth. As a result, pH can affect most of the equilibria involved in the process [109]. At a certain pH, for example, the surface charge can be reduced to zero; this is known as the isoelectric point [68]. Several studies [6,68,110] have confirmed that pH plays an important role in controlling the size and formation of NPs. Temperature is a physical parameter that affects the spatial and dimensional distribution of particles [111,112]. As the reaction temperature rises, so does the rate of metal ion reduction [113,114], and at 70 °C, smaller nanoparticles are formed with the help of *Canna indica* extracts. The high temperature promotes the rapid conversion of the metallic solution into nanoparticles, whereas at room temperature, the synthesis takes longer [111,115]. The kinetic energy of the reactants increases as the temperature rises. The rapid reduction of metal cations accelerates the formation of nanoparticles by increasing the formation of nucleation centers [116]. Furthermore, the high temperature causes the formation of more stable and smaller nanoparticles. It has also been reported that the absorbance of nanoparticles increases with temperature, indicating that the nanoparticles are highly concentrated. However, the temperature must be kept between 30 and 100 degrees Celsius because phytochemicals decompose at higher temperatures, interfering with the critical reduction process [114]. Because the reduction reaction, regardless of the extract used, cannot occur instantly, biosynthesis time is an important parameter to consider [117]. Another critical factor is the initial concentration of metal ions in the reaction mixture [26]. Because of the availability of functional groups in the extract compounds, a concentration of 1 mM causes a rapid metal reduction [118].

The produced nanoparticles formed chain-like clusters as a result of magnetic and electrostatic interactions, and the compositions of each nanoparticle did not disclose two separate phases due to agglomeration, as shown in Figure 7. The bimetallic Fe/Cu nanoparticles formed a non-homogeneous variety of cluster close to spherical nanoparticles that lacked specified geometrical shape of various sizes, regardless of the reduction agent utilized during production. Similarly, Manickam-Periyaraman, et al. [119] discovered a non-homogeneous diversity of cubic, polyhedral, and NPs lacking specified geometrical shape of various sizes in bimetallic iron-copper oxide nanoparticles. This was also observed in a study by de França Bettencourt, et al. [120], where TEM images of NPs exhibiting

spherical morphology and agglomeration were observed. On the contrary, according to the TEM images of Zin, et al. [121], iron particle nanoparticles with the least amount of a second metal, copper, show the least agglomeration among the synthesized particles, while the TEM images of the as-synthesized nanoparticles show spherical particles, with sizes ranging from 30 to 50 nm in a study by Fang, et al. [122].

For each flocculant to flocculate maximally an optimal dosage is required. Beyond this dosage, decline in flocculation activity may be observed as a result of destabilized flocs by excess polymer. Contrary to this, no significant bridging that occurs between colloids and polymeric flocculant below optimal dosage was observed [123]. The amount of flocculant required for optimal flocculation activity is defined as dosage size. In the present study, flocculation activity of different concentration of nanoparticles (0.2–0.8 mg/mL) was investigated, with kaolin as the test material. From Table 3, it can be observed that highest flocculation activity was 99% at 0.2 mg/mL, followed by 98% for both 0.4 and 0.6 mg/mL, and the least was at 0.8 mg/mL, with 93% flocculation activity. However, among 0.2, 0.4, and 0.6 mg/mL there was no statistical significance observed, suggesting that any of the three dosages was effective. Therefore, to save the flocculant, 0.2 mg/mL was chosen for all subsequent experiments. The decreased flocculation activity at 0.8 mg/mL could be attributed to kaolin binding site blockage by excess flocculant.

By reducing the negative charge of the polymer and the particles, cations promote the action of bioflocculant adsorption on the suspended kaolin particles. The negative charge of the functional groups in a solution's bioflocculant and colloidal kaolin particles is stabilized and neutralized by cations [54]. In the presence of trivalent, divalent, and monovalent cations, it was discovered that the synthesized BNPs did not flocculate well. However, the nanoparticles could still flocculate, with over 95% flocculation activity in the absence of cation addition (control), indicating that cation addition is not required when employing these nanoparticles. Thus, it may be said that the nanoparticles have value for industry.

The flocculation activity is impacted by  $H^+$  ions concentration. This impact can have an influence on the stability of colloids and, consequently, floc formation. The pH of the reaction mixture is one of the factors affecting the flocculation process [62]. From Table 3, nanoparticles were shown not to be affected by a change in pH, as the flocculation activity was above 95% at all pH levels investigated. The findings suggest that bimetallic nanoparticles are of commercial value in terms of their application in wastewater with different pH values. The flocculation activity of nanoparticles after they were subjected at different temperatures was investigated. The nanoparticles were heated for 30 min at 60, 80, and 100 °C before they were used as a flocculating agent. This was carried out to determine the thermostability of the nanoparticles. As shown in Table 3, the nanoparticles proved to be thermostable, as they were not affected by temperature variation. Flocculation activity remained above 90%. However, at room temperature (27 °C), the flocculation activity was 99%, indicating that the mixture does not require temperature adjustment for nanoparticles to be effective. Although at 60 °C there was slightly drop in flocculation activity from 99 to 93%, there was no statistical significance among these temperature, as indicated in Table 3. It was, therefore, concluded that the synthesized nanoparticles are thermostable.

Materials with desired properties that have better catalytic activity which cannot be achieved by a single-metal atom can be obtained by the use of bimetallic nanoparticles [6]. Interesting chemical, electronic, biological, mechanical, and thermal properties have been unveiled by bimetallic nanoparticles due to the synergistic effects and composition. The specific properties of bimetallic nanoparticles are enhanced by a combination of two different metals, and these properties may differ from those of pure element particles. Bimetallic nanoparticles have been used as the antimicrobial agent, and they have been found to be more effective than single metallic nanoparticles [85]. Bimetallic nanoparticles also serve as great antimicrobials, and they can complement the role of antibiotics in combating bacteria. These nanoparticles can either produce ROS (reactive oxygen species)

that cause DNA disruption, or they can interfere with bacterial growth either by disrupting their membrane, which can also hinder its protein functioning machinery [124].

In the study conducted by Dlamini, Basson, Shandu, Mavuso and Pullabhotla [32], nanoparticles exhibited antimicrobial activity against a Gram-positive bacterium *Bacillus subtilis* CSM5 and a Gram-negative bacterium *E. coli* ATCC 25922. Similarly, Zhao, Ye, Liu, Chen and Jiang [85] alluded that Au/Pt bimetallic nanoparticles have antimicrobial activity against *E. coli*. In another study where bimetallic nanoparticles (Ag/Au) were compared to single metallic nanoparticles (Ag NPs and Au NPs), it was revealed that the single metallic nanoparticles did not have activity against *Salmonella typhi* and *E. coli*, while bimetallic did have activity against these microorganisms. Furthermore, good antibacterial activity against Gram-negative bacteria *Klebsiella pneumoniae* and Gram-positive bacteria *Staphylococcus aureus* was exhibited by the bimetallic nanoparticles [74]. In another study, where BNPs (Au/Ag) were synthesized from *Oscimum basilicum* (Basil) flower and leaf extracts, they showed antimicrobial activity against *Staphylococcus aureus*, *Pseudomonas aeruginosa*, *E. coli*, and *Bacillus subtilis* [75]. Synergistic effects of Ag-Cu BNPs and antibiotics were evaluated by Nazeruddin, Prasad, Shaikh and Shaikh [76], and it was found that the nanoparticles have activity against Gram-positive bacteria *Bacillus subtilis*. The study concluded that BNPs synergistic effects with antibiotics and sulpha drugs can be exploited for the preparation of medicine against bacteria.

A promising research field for this bimetallic nanoparticles is treatment of water and wastewater due to its catalytic properties, and high efficiency is achieved [89]. Through the mechanism of adsorption, advanced oxidation, reduction, as well as oxidation or a combination of these, bimetallic systems can remove inorganic, organic, and heavy metal contaminants [125]. Bimetallic catalyst demonstrated to be appropriate for increasing selectivity activity, upgrading catalytic activity, limiting the expense of catalysts, and enhancing stability. Bimetallic nanoparticles surmounted most of the limitations that monometallic nanoparticles were facing.

Under anaerobic and aerobic circumstances, the impact of various nanoparticle concentrations on COD removal was studied. The results of the experiment showed that after 96 h of exposure to 500 mg/L bimetallic nanoparticles, the COD elimination effectiveness approaches 86% [79]. In addition, it was discovered that anaerobic conditions accelerated the elimination of COD in comparison with aerobic ones. On the basis of these observations, the various mechanisms for COD degradation were hypothesized, including adsorption and reductive reaction. While the reductive reaction approach is attributed to the reactant of bimetallic Cu/NZVI to directly serve, the adsorption technique involves absorbing organic matter onto the surface of bimetallic nanoparticles. The reductive reaction strategy is proposed while the corrosion of bimetallic particle emits two electrons that will be transferred to the organic matter. In another study conducted by Dlamini, Basson and Pullabhotla [83], where the effect of Fe/Cu BNPs in COD removal on coal mine wastewater was investigated, it was shown that the bimetallic nanoparticles are effective in removing up to 88% COD after 1 h when 0.2 mg/mL concentration of nanoparticles was used. Furthermore, the Fe/Cu BNPs proved to have high BOD removal efficacy of 96% after five days. Contrary to this, when zero-valent iron nanoparticles were applied in BOD removal, the efficacy was 60.31% [126]. This comparison proves that bimetallic nanoparticles are more effective in wastewater treatment than monometallic nanoparticles.

For the normal functioning of the ecosystem, phosphorus (P) is an important nutrient. Nonetheless, excess of nitrogen (N) and P is the main eutrophication cause [127]. Agriculture and domestic wastewater have the main input of P in nature [128]. Due to continuing eutrophication, governmental regulation of P in freshwater ecosystems has increased. From Table 5, the Fe/Cu BNPs could remove total nitrogen and phosphate effectively from river water. As indicated, 94% of total nitrogen was removed after 3 h, while only 40% of phosphate was removed when the reaction was left for 3 h; however, when the contact time was increased to 1 week, 99% phosphate was removed, indicating that contact time is the important factor in phosphate removal.

The large amount of wastewater that needs to be treated before being released back to the environment has increased due to the growth of agriculture and industrial activities. Due to low retention by soil particles and high solubility in water, nitrate ( $\text{NO}_3^-$ ) is the most diffused contaminant [129]. In agricultural regions, contamination by  $\text{NO}_3^-$  is due to application of fertilizer and animal farming [130], atmospheric deposition, septic tanks, and industrial and wastewater discharges [131]. The amount of water in the soil and the characteristics of the soil determine how quickly nitrate leaches into subsurface layers and ultimately into groundwater if it is not taken up by plants or denitrified into  $\text{N}_2\text{O}$  and  $\text{N}_2$  [132]. Nitrates are a vital source of mineral nitrogen for plants, but they are hazardous to people because they are reduced into nitrites, which then react with amino acids or amines to generate nitrosamines, which are known to be mutagenic and carcinogenic substances [133]. Nitrates have also been linked to a range of health problems, including immune system alterations, spontaneous abortion, central nervous system damage, hypertension, birth abnormalities, diabetes, respiratory tract infection, and hypertension [132,134]. World Health Organization (WHO) has set the maximum contaminant level (MCL) at  $50 \text{ mg NO}_3^- \text{ L}^{-1}$  and  $11.3 \text{ mg N L}^{-1}$  [134]. There are various techniques that have been proven to be effective in removing nitrate contaminants, such as reverse osmosis, ion exchange, and electrodialysis. The implementation of these techniques on a large scale is limited due to high energy consumption, nitrate brine concentration, technological complexity, and secondary pollution [135].

Due to the rapid rise of industrialisation, the environment became contaminated with harmful metals from wastewater. Due to the non-degradability of heavy metals and their toxicity even at low concentrations, heavy metal treatment is a major concern. These pollutants pose a severe risk to living organisms and the environment if they are accumulated [136]. Hence, treatment of effluents from industries containing toxic metals is crucial before they are discharged [137]. As indicated in Table 5, CuNi bimetallic showed remarkable properties with high removal efficacy for  $\text{Pb}^{2+}$ ,  $\text{Cd}^{2+}$ , and  $\text{Zn}^{2+}$  with 100, 98.34, and 91.42% removal efficiency, respectively [80]. Increased use of organic pollutants in agriculture and industries has led to environmental safety becoming a serious problem in the scientific field. In our environment, organic pollutants have significant adverse effects. Among the frequently used and discharged pollutants into the environment are organic contaminants and dyes [138,139]. Dye industries contribute significantly to the development of any country. There are 10,000 tons of commercially available dyes, 700,000 tons are manufactured per annum [140,141], and 10–15% of the total dyestuff is discharged into natural environment [142]. Due to their complex chemical structure and synthetic origin, dyes are persistent in nature [143], and a large number of dyes are carcinogenic in nature and composed of aromatic compounds [144].

In addition to dyes, phenolic chemicals from industrial effluents are regarded as persistent. These contaminants are found in wastewater from several businesses, including those that produce plastics, paint, textiles, leather, rubbers, steel, pesticides, dyes, olives, pulp, medicines, and paper [145–147]. The elimination of these toxins from wastewater becomes a major concern since they affect people's quality of life. In addition to these, it also results in chest pain, nausea, throat burning, and chest itching and burning. Due of its numerous detrimental health impacts, some nations have banned and regulated its usage in food goods. However, RhB is still being used illegally in the food industry and other sectors because of its low production costs, great stability, and color fastness [148]. RhB should not be dumped into bodies of water due to its negative effects on health. Therefore, it is crucial to develop creative methods for lowering and degrading RhB.

## 5. Conclusions

In this review, we summarized various bimetallic nanoparticle synthesis methods, factors affecting their synthesis, mechanisms of formation, and their various applications. So far, various fabrication strategies have been developed for the support of bimetallic nanoparticle synthesis, which can generally be divided into three classes: physical, chemical,

and biological. In biological synthesis, plant extract, microorganism extract (biofloculant), starch, and microorganisms are some of the techniques reported in the literature. While the chemical method involves the use of a reducing agent, such as sodium borohydride, in an aqueous solution to create metal nanoparticles, chemical reduction is the simplest method for producing metal nanoparticles, but it has several drawbacks, including toxicity, expense, poor reducing ability, and impurities. The physical method has been reported to have its advantages, which include no solvent contamination in the prepared film and uniformity in the formation of nanoparticles; however, there were some drawbacks reported as well, and these include methods that necessitate the purchase of expensive equipment and a low final yield. Furthermore, different characterization techniques for bimetallic nanoparticles are reported. This includes X-ray diffraction (XRD) to investigate crystallinity and phase composition; the morphology and composition analysis of nanoparticles are studied using a scanning electron microscope fitted with an energy-dispersive X-ray analyzer (EDX); transmission electron microscopy (TEM), UV-vis spectrum, FTIR, and TGA analysis are also among the characterization tools used. From the literature, the presence of an iron amorphous phase was indicated by the broad peak at 2 in X-ray diffraction patterns, while the infrared spectrum bands provide information about many chemicals surrounding Fe/Cu nanoparticles, such as amides, alcohols, and proteins. The bimetallic nanoparticles have been reported to have various applications in different fields. These include antimicrobial activity, wastewater treatment, and pollutant removal, among others. In wastewater treatment, it has been reported that the bimetallic nanoparticles could flocculate up to 99% at a dosage of 0.2 mg/mL. For antimicrobial activity, different bimetallic nanoparticles proved to be effective against pathogenic microorganisms, which include, among others, *Escherichia coli*, *Bacillus pumilus A. freundii*, *Klebsiella pneumoniae*, *Scholeraesius*, *Salmonella typhi*, *Staphylococcus aureus*, and *Pseudomonas aeruginosa*. Because of synergistic effects and composition, bimetallic nanoparticles have revealed intriguing chemical, electronic, biological, mechanical, and thermal properties. Bimetallic nanoparticles have enhanced properties due to the combination of two different metals, and these properties may differ from those of pure element particles. BNPs were discovered to be effective at removing pollutants (nitrate, BOD, and COD) from wastewater. As demonstrated by the preceding discussion, bimetallic nanoparticles are multifunctional nanomaterials with applications in a variety of industries. The “synergistic effect” that the two metals have when combined results in multifunctionality. Researchers are synthesizing an increasing number of new BNPs with specific geometrical and magnetic properties. Another argument is that bimetallic nanoparticles are more important than monometallic nanoparticles due to their superior properties. Recommendation and prospects: biological methods are the most recommended method for synthesis of nanoparticles. Green synthesis is an efficient alternative to physical and chemical methods because it is nontoxic, cost effective, provides rapid synthesis, is eco-friendly, monodispersed, produces little waste, and can be produced on a large scale.

**Author Contributions:** Conceptualization, A.K.B. and V.S.R.P.; formal analysis, N.G.D. and V.S.R.P.; investigation, N.G.D.; supervision, A.K.B. and V.S.R.P.; writing—original draft, N.G.D.; writing—review and editing, V.S.R.P. All authors have read and agreed to the published version of the manuscript.

**Funding:** Rajasekhar Pullabhotla would like to acknowledge the National Research Foundation (NRF, South Arica) for their financial support in the form of the Incentive Fund Grant (grant no. 103691) and the Research Developmental Grant for Rated Researchers (112145).

**Institutional Review Board Statement:** Not applicable.

**Informed Consent Statement:** Not applicable.

**Data Availability Statement:** Data sharing not applicable.

**Acknowledgments:** Nkosinathi Dlamini would like to acknowledge the Council for Scientific and Industrial Research (CSIR, South Africa) for the financial assistance in the form of the Doctoral bursary. The authors (Dlamini, N.G, Basson, A.K and Pullabhotla, V.S.R) would like to acknowledge the Electron Microscopy Unit at the University of KwaZulu-Natal, Westville campus, for providing support by letting us use the TEM and SEM-EDX facilities for the characterization of nanomaterials.

**Conflicts of Interest:** The authors declare that there are no conflict of interest.

## References

1. Duan, M.; Jiang, L.; Zeng, G.; Wang, D.; Tang, W.; Liang, J.; Wang, H.; He, D.; Liu, Z.; Tang, L. Bimetallic nanoparticles/metal-organic frameworks: Synthesis, applications and challenges. *Appl. Mater. Today* **2020**, *19*, 100564. [[CrossRef](#)]
2. Medina-Cruz, D.; Saleh, B.; Vernet-Crua, A.; Nieto-Argüello, A.; Lomelí-Marroquín, D.; Vélez-Escamilla, L.Y.; Cholula-Díaz, J.L.; García-Martín, J.M.; Webster, T. Bimetallic nanoparticles for biomedical applications: A review. In *Racing for the Surface*; Springer: Berlin, Germany, 2020; pp. 397–434.
3. Scala, A.; Neri, G.; Micale, N.; Cordaro, M.; Piperno, A. State of the Art on Green Route Synthesis of Gold/Silver Bimetallic Nanoparticles. *Molecules* **2022**, *27*, 1134. [[CrossRef](#)]
4. Li, H.; He, Z.; Ouyang, Z.; Palchoudhury, S.; Ingram, C.W.; Harruna, I.I.; Li, D. Modifying electrical and magnetic properties of single-walled carbon nanotubes by decorating with iron oxide nanoparticles. *J. Nanosci. Nanotechnol.* **2020**, *20*, 2611–2616. [[CrossRef](#)] [[PubMed](#)]
5. He, Z.; Zhang, Z.; Bi, S. Nanoparticles for organic electronics applications. *Mater. Res. Express* **2020**, *7*, 012004. [[CrossRef](#)]
6. Sharma, G.; Kumar, A.; Sharma, S.; Naushad, M.; Dwivedi, R.P.; AlOthman, Z.A.; Mola, G.T. Novel development of nanoparticles to bimetallic nanoparticles and their composites: A review. *J. King Saud Univ. Sci.* **2019**, *31*, 257–269. [[CrossRef](#)]
7. Ferrando, R.; Jellinek, J. Nano-particles as a catalysts incatalytic converters, RL Johnston. *Chem. Rev.* **2009**, *108*, 845. [[CrossRef](#)]
8. Kumar, R.; Mondal, K.; Panda, P.K.; Kaushik, A.; Abolhassani, R.; Ahuja, R.; Rubahn, H.-G.; Mishra, Y.K. Core-shell nanostructures: Perspectives towards drug delivery applications. *J. Mater. Chem. B* **2020**, *8*, 8992–9027. [[CrossRef](#)]
9. Liu, W.-J.; Qian, T.-T.; Jiang, H. Bimetallic Fe nanoparticles: Recent advances in synthesis and application in catalytic elimination of environmental pollutants. *Chem. Eng. J.* **2014**, *236*, 448–463. [[CrossRef](#)]
10. Moudgil, A.; Chaudhari, B.P. Fungi the crucial contributors for nanotechnology: A green chemistry perspective. In *Advancing Frontiers in Mycology & Mycotechnology*; Springer: Berlin, Germany, 2019; pp. 279–298.
11. Verma, A.; Gautam, S.P.; Bansal, K.K.; Prabhakar, N.; Rosenholm, J.M. Green nanotechnology: Advancement in phytoformulation research. *Medicines* **2019**, *6*, 39. [[CrossRef](#)]
12. Couvreur, P. Nanoparticles in drug delivery: Past, present and future. *Adv. Drug Deliv. Rev.* **2013**, *65*, 21–23. [[CrossRef](#)]
13. Stolyar, S.; Balaev, D.; Ladygina, V.; Dubrovskiy, A.; Krasikov, A.; Popkov, S.; Bayukov, O.; Knyazev, Y.V.; Yaroslavtsev, R.; Volochaev, M. Bacterial ferrihydrite nanoparticles: Preparation, magnetic properties, and application in medicine. *J. Supercond. Nov. Magn.* **2018**, *31*, 2297–2304. [[CrossRef](#)]
14. Gong, H.; Li, Z.; Chen, Z.; Liu, Q.; Song, M.; Huang, C. NiSe/Cd<sub>0.5</sub>Zn<sub>0.5</sub>S composite nanoparticles for use in p–n heterojunction-based photocatalysts for solar energy harvesting. *ACS Appl. Nano Mater.* **2020**, *3*, 3665–3674. [[CrossRef](#)]
15. Bhalla, V.; Tyagi, H. Solar energy harvesting by cobalt oxide nanoparticles, a nanofluid absorption based system. *Sustain. Energy Technol. Assess.* **2017**, *24*, 45–54. [[CrossRef](#)]
16. Schwarz, J.A.; Contescu, C.I.; Putyera, K. *Dekker Encyclopedia of Nanoscience and Nanotechnology*; CRC Press: Boca Raton, FL, USA, 2004; Volume 5.
17. Nasrollahzadeh, M.; Sajjadi, M.; Irvani, S.; Varma, R.S. Trimetallic nanoparticles: Greener synthesis and their applications. *Nanomaterials* **2020**, *10*, 1784. [[CrossRef](#)] [[PubMed](#)]
18. Hasan, S. A review on nanoparticles: Their synthesis and types. *Res. J. Recent Sci.* **2015**, 2277, 2502.
19. Irvani, S.; Varma, R.S. Bacteria in heavy metal remediation and nanoparticle biosynthesis. *ACS Sustain. Chem. Eng.* **2020**, *8*, 5395–5409. [[CrossRef](#)]
20. Vajtai, R. *Springer Handbook of Nanomaterials*; Springer Science & Business Media: Berlin, Germany, 2013.
21. Sharma, G.; Kumar, D.; Kumar, A.; Ala'a, H.; Pathania, D.; Naushad, M.; Mola, G.T. Revolution from monometallic to trimetallic nanoparticle composites, various synthesis methods and their applications: A review. *Mater. Sci. Eng. C* **2017**, *71*, 1216–1230. [[CrossRef](#)]
22. Ghosh Chaudhuri, R.; Paria, S. Core/shell nanoparticles: Classes, properties, synthesis mechanisms, characterization, and applications. *Chem. Rev.* **2012**, *112*, 2373–2433. [[CrossRef](#)]
23. Srdić, V.V.; Mojić, B.; Nikolić, M.; Ognjanović, S. Recent progress on synthesis of ceramics core/shell nanostructures. *Process. Appl. Ceram.* **2013**, *7*, 45–62. [[CrossRef](#)]
24. Nomoev, A.V.; Bardakhanov, S.P.; Schreiber, M.; Bazarova, D.G.; Romanov, N.A.; Baldanov, B.B.; Radnaev, B.R.; Syzrantsev, V.V. Structure and mechanism of the formation of core-shell nanoparticles obtained through a one-step gas-phase synthesis by electron beam evaporation. *Beilstein J. Nanotechnol.* **2015**, *6*, 874–880. [[CrossRef](#)]

25. Fakhri, A.; Tahami, S.; Naji, M. Synthesis and characterization of core-shell bimetallic nanoparticles for synergistic antimicrobial effect studies in combination with doxycycline on burn specific pathogens. *J. Photochem. Photobiol. B Biol.* **2017**, *169*, 21–26. [[CrossRef](#)] [[PubMed](#)]
26. Dlamini, N.G.; Basson, A.K.; Shandu, J.S.; Pullabhotla, V.S.R. Optimization of Fe@Cu core-shell nanoparticle synthesis, characterization, and application in dye removal and wastewater treatment. *Catalysts* **2020**, *10*, 755. [[CrossRef](#)]
27. Dhand, C.; Dwivedi, N.; Loh, X.J.; Ying, A.N.J.; Verma, N.K.; Beuerman, R.W.; Lakshminarayanan, R.; Ramakrishna, S. Methods and strategies for the synthesis of diverse nanoparticles and their Applications: A comprehensive overview. *RSC Adv.* **2015**, *5*, 105003–105037. [[CrossRef](#)]
28. Parveen, K.; Banse, V.; Ledwani, L. Green synthesis of nanoparticles: Their advantages and disadvantages. In *AIP Conference Proceedings*; AIP Publishing LLC: Melville, NY, USA, 2016; p. 020048.
29. Dlamini, N.G.; Basson, A.K.; Pullabhotla, V.S.R. Optimization and application of biofloculant passivated copper nanoparticles in the wastewater treatment. *Int. J. Environ. Res. Public Health* **2019**, *16*, 2185. [[CrossRef](#)]
30. Schulte, J. *Nanotechnology: Global Strategies, Industry Trends and Applications*; John Wiley & Sons: Hoboken, NJ, USA, 2005.
31. Thomas, K.; Sayre, P. Research strategies for safety evaluation of nanomaterials, Part I: Evaluating the human health implications of exposure to nanoscale materials. *Toxicol. Sci.* **2005**, *87*, 316–321. [[CrossRef](#)]
32. Dlamini, N.G.; Basson, A.K.; Shandu, J.; Mavuso, S.S.; Pullabhotla, V.S.R. Biosynthesis, characterization, and application of iron nanoparticles: In dye removal and as antimicrobial agent. *Water Air Soil Pollut.* **2020**, *231*, 130.
33. Jiang, D.; Huang, D.; Lai, C.; Xu, P.; Zeng, G.; Wan, J.; Tang, L.; Dong, H.; Huang, B.; Hu, T. Difunctional chitosan-stabilized Fe/Cu bimetallic nanoparticles for removal of hexavalent chromium wastewater. *Sci. Total Environ.* **2018**, *644*, 1181–1189. [[CrossRef](#)]
34. Kefeni, K.K.; Msagati, T.A.; Nkambule, T.T.; Mamba, B.B. Synthesis and application of hematite nanoparticles for acid mine drainage treatment. *J. Environ. Chem. Eng.* **2018**, *6*, 1865–1874. [[CrossRef](#)]
35. Weng, X.; Jin, X.; Lin, J.; Naidu, R.; Chen, Z. Removal of mixed contaminants Cr (VI) and Cu (II) by green synthesized iron based nanoparticles. *Ecol. Eng.* **2016**, *97*, 32–39. [[CrossRef](#)]
36. Sánchez-López, E.; Gomes, D.; Esteruelas, G.; Bonilla, L.; Lopez-Machado, A.L.; Galindo, R.; Cano, A.; Espina, M.; Ettcheto, M.; Camins, A. Metal-based nanoparticles as antimicrobial agents: An overview. *Nanomaterials* **2020**, *10*, 292. [[CrossRef](#)]
37. Meddahi-Pellé, A.; Legrand, A.; Marcellan, A.; Louedec, L.; Letourneur, D.; Leibler, L. Organ repair, hemostasis, and in vivo bonding of medical devices by aqueous solutions of nanoparticles. *Angew. Chem. Int. Ed.* **2014**, *53*, 6369–6373. [[CrossRef](#)] [[PubMed](#)]
38. Ravishankar, R.V.; Jamuna, B.A. Nanoparticles and Their Potential Application as Antimicrobials. In *Science against Microbial Pathogens: Communicating Current Research and Technological Advances*; No. 3; Méndez-Vilas, A., Ed.; Microbiology Series Formatex Research Center: Madrid, Spain, 2011; Volume 1, pp. 197–209.
39. Nairn, J.J.; Shapiro, P.J.; Twamley, B.; Pounds, T.; Von Wandruszka, R.; Fletcher, T.R.; Williams, M.; Wang, C.; Norton, M.G. Preparation of ultrafine chalcopyrite nanoparticles via the photochemical decomposition of molecular single-source precursors. *Nano Lett.* **2006**, *6*, 1218–1223. [[CrossRef](#)] [[PubMed](#)]
40. Cele, T. Preparation of nanoparticles. *Eng. Nanomater. Health Saf.* **2020**, 15–25. [[CrossRef](#)]
41. Katwal, R.; Kaur, H.; Sharma, G.; Naushad, M.; Pathania, D. Electrochemical synthesized copper oxide nanoparticles for enhanced photocatalytic and antimicrobial activity. *J. Ind. Eng. Chem.* **2015**, *31*, 173–184. [[CrossRef](#)]
42. Anandgaonker, P.; Kulkarni, G.; Gaikwad, S.; Rajbhoj, A. Synthesis of TiO<sub>2</sub> nanoparticles by electrochemical method and their antibacterial application. *Arab. J. Chem.* **2019**, *12*, 1815–1822. [[CrossRef](#)]
43. Khan, Z.; Al-Thabaiti, S.A.; Obaid, A.Y.; Al-Youbi, A. Preparation and characterization of silver nanoparticles by chemical reduction method. *Colloids Surf. B Biointerfaces* **2011**, *82*, 513–517. [[CrossRef](#)]
44. Dang, T.M.D.; Le, T.T.T.; Fribourg-Blanc, E.; Dang, M.C. Synthesis and optical properties of copper nanoparticles prepared by a chemical reduction method. *Adv. Nat. Sci. Nanosci. Nanotechnol.* **2011**, *2*, 015009. [[CrossRef](#)]
45. Anandan, S.; Grieser, F.; Ashokkumar, M. Sonochemical synthesis of Au–Ag core–shell bimetallic nanoparticles. *J. Phys. Chem. C* **2008**, *112*, 15102–15105. [[CrossRef](#)]
46. Minisha, S.; Vedhi, C.; Rajakani, P. Methods of Graphene Synthesis and Graphene-Based Electrode Material for Supercapacitor Applications. *ECS J. Solid State Sci. Technol.* **2022**, *11*, 111002. [[CrossRef](#)]
47. Acsente, T.; Negrea, R.F.; Nistor, L.C.; Logofatu, C.; Matei, E.; Birjega, R.; Grisolia, C.; Dinescu, G. Synthesis of flower-like tungsten nanoparticles by magnetron sputtering combined with gas aggregation. *Eur. Phys. J. D* **2015**, *69*, 161. [[CrossRef](#)]
48. Zorkipli, N.N.M.; Kaus, N.H.M.; Mohamad, A.A. Synthesis of NiO nanoparticles through sol-gel method. *Procedia Chem.* **2016**, *19*, 626–631. [[CrossRef](#)]
49. Devarajan, S.; Bera, P.; Sampath, S. Bimetallic nanoparticles: A single step synthesis, stabilization, and characterization of Au–Ag, Au–Pd, and Au–Pt in sol–gel derived silicates. *J. Colloid Interface Sci.* **2005**, *290*, 117–129. [[CrossRef](#)] [[PubMed](#)]
50. Abbaspour, A.; Norouz-Sarvestani, F. High electrocatalytic effect of Au–Pd alloy nanoparticles electrodeposited on microwave assisted sol–gel-derived carbon ceramic electrode for hydrogen evolution reaction. *Int. J. Hydrogen Energy* **2013**, *38*, 1883–1891. [[CrossRef](#)]
51. Gołębiewska, A.; Lisowski, W.; Jarek, M.; Nowaczyk, G.; Michalska, M.; Jurga, S.; Zaleska-Medynska, A. The effect of metals content on the photocatalytic activity of TiO<sub>2</sub> modified by Pt/Au bimetallic nanoparticles prepared by sol-gel method. *Mol. Catal.* **2017**, *442*, 154–163. [[CrossRef](#)]

52. Sharma, G.; Kumar, A.; Naushad, M.; Pathania, D.; Sillanpää, M. Polyacrylamide@ Zr (IV) vanadophosphate nanocomposite: Ion exchange properties, antibacterial activity, and photocatalytic behavior. *J. Ind. Eng. Chem.* **2016**, *33*, 201–208. [[CrossRef](#)]
53. Devi, R.A.; Latha, M.; Velumani, S.; Oza, G.; Reyes-Figueroa, P.; Rohini, M.; Becerril-Juarez, I.; Lee, J.-H.; Yi, J. Synthesis and characterization of cadmium sulfide nanoparticles by chemical precipitation method. *J. Nanosci. Nanotechnol.* **2015**, *15*, 8434–8439. [[CrossRef](#)]
54. Maliehe, T.S.; Basson, A.K.; Dlamini, N.G. Removal of pollutants in mine wastewater by a non-cytotoxic polymeric biofloculant from *Alcaligenes faecalis* HCB2. *Int. J. Environ. Res. Public Health* **2019**, *16*, 4001. [[CrossRef](#)]
55. Mehta, B.; Chhajlani, M.; Shrivastava, B. Green synthesis of silver nanoparticles and their characterization by XRD. In *Journal of Physics: Conference Series*; IOP Publishing: Bristol, UK, 2017; p. 012050.
56. Hossain, M.A.; Islam, S. Synthesis of carbon nanoparticles from kerosene and their characterization by SEM/EDX, XRD and FTIR. *Am. J. Nanosci. Nanotechnol.* **2013**, *1*, 52. [[CrossRef](#)]
57. Kaasalainen, M.; Aseyev, V.; von Haartman, E.; Karaman, D.Ş.; Mäkilä, E.; Tenhu, H.; Rosenholm, J.; Salonen, J. Size, stability, and porosity of mesoporous nanoparticles characterized with light scattering. *Nanoscale Res. Lett.* **2017**, *12*, 74. [[CrossRef](#)] [[PubMed](#)]
58. León, A.; Reuquen, P.; Garín, C.; Segura, R.; Vargas, P.; Zapata, P.; Orihuela, P.A. FTIR and Raman characterization of TiO<sub>2</sub> nanoparticles coated with polyethylene glycol as carrier for 2-methoxyestradiol. *Appl. Sci.* **2017**, *7*, 49. [[CrossRef](#)]
59. Teoh, L.G.; Li, K.-D. Synthesis and characterization of NiO nanoparticles by sol–gel method. *Mater. Trans.* **2012**, *53*, 2135–2140. [[CrossRef](#)]
60. Begum, R.; Farooqi, Z.H.; Naseem, K.; Ali, F.; Batool, M.; Xiao, J.; Irfan, A. Applications of UV/Vis spectroscopy in characterization and catalytic activity of noble metal nanoparticles fabricated in responsive polymer microgels: A review. *Crit. Rev. Anal. Chem.* **2018**, *48*, 503–516. [[CrossRef](#)] [[PubMed](#)]
61. Kurane, R.; Toeda, K.; Takeda, K.; Suzuki, T. Culture conditions for production of microbial flocculant by *Rhodococcus erythropolis*. *Agric. Biol. Chem.* **1986**, *50*, 2309–2313.
62. Eloff, J.N. A sensitive and quick microplate method to determine the minimal inhibitory concentration of plant extracts for bacteria. *Planta Med.* **1998**, *64*, 711–713. [[CrossRef](#)] [[PubMed](#)]
63. Maliehe, T.S.; Shandu, J.S.; Basson, A.K. The antibacterial and antidiarrheal activities of the crude methanolic *Syzygium cordatum* [S. Ncik, 48 (UZ)] fruit pulp and seed extracts. *J. Med. Plants Res.* **2015**, *9*, 884–891. [[CrossRef](#)]
64. Anitasari, S.; Ismail, S.; Wiratama, B.S.; Budi, H.S. Antibacterial and Phytochemical Analysis of Two Plants Menispermaceae Family. *Syst. Rev. Pharm.* **2020**, *11*, 150–156.
65. Mahdavi, B.; Paydarfard, S.; Rezaei-Seresht, E.; Baghayeri, M.; Nodehi, M. Green synthesis of NiONPs using *Trigonella subenervis* extract and its applications as a highly efficient electrochemical sensor, catalyst, and antibacterial agent. *Appl. Organomet. Chem.* **2021**, *35*, e6264. [[CrossRef](#)]
66. Pan, C.-J.; Sarma, L.S.; Hwang, B.-J. Formation and characterization of bimetallic nanoparticles in electrochemistry. In *Handbook of Nanoelectrochemistry*; Springer: Berlin, Germany, 2016; pp. 169–239.
67. Behera, A.; Mittu, B.; Padhi, S.; Patra, N.; Singh, J. Bimetallic nanoparticles: Green synthesis, applications, and future perspectives. In *Multifunctional Hybrid Nanomaterials for Sustainable Agri-Food and Ecosystems*; Elsevier: Amsterdam, The Netherlands, 2020; pp. 639–682.
68. Berta, L.; Coman, N.-A.; Rusu, A.; Tanase, C. A Review on Plant-Mediated Synthesis of Bimetallic Nanoparticles, Characterisation and Their Biological Applications. *Materials* **2021**, *14*, 7677. [[CrossRef](#)]
69. Dlamini, N.G.; Basson, A.K.; Pullabhotla, V.S.R. A Comparative study between Bimetallic Iron@ copper nanoparticles with iron and copper nanoparticles synthesized Using a biofloculant: Their applications and biosafety. *Processes* **2020**, *8*, 1125. [[CrossRef](#)]
70. Tushima, N.; Yonezawa, T. Bimetallic nanoparticles—Novel materials for chemical and physical applications. *New J. Chem.* **1998**, *22*, 1179–1201. [[CrossRef](#)]
71. Schabes-Retchkiman, P.; Canizal, G.; Herrera-Becerra, R.; Zorrilla, C.; Liu, H.; Ascencio, J. Biosynthesis and characterization of Ti/Ni bimetallic nanoparticles. *Opt. Mater.* **2006**, *29*, 95–99. [[CrossRef](#)]
72. He, F.; Zhao, D. Preparation and characterization of a new class of starch-stabilized bimetallic nanoparticles for degradation of chlorinated hydrocarbons in water. *Environ. Sci. Technol.* **2005**, *39*, 3314–3320. [[CrossRef](#)] [[PubMed](#)]
73. Castro-Longoria, E.; Vilchis-Nestor, A.R.; Avalos-Borja, M. Biosynthesis of silver, gold and bimetallic nanoparticles using the filamentous fungus *Neurospora crassa*. *Colloids Surf. B Biointerfaces* **2011**, *83*, 42–48. [[CrossRef](#)] [[PubMed](#)]
74. Ramakritinan, C.; Kaarunya, E.; Shankar, S.; Kumaraguru, A. Antibacterial effects of Ag, Au and bimetallic (Ag-Au) nanoparticles synthesized from red algae. In *Solid State Phenomena*; Trans Tech Publications Ltd.: Stafa-Zurich, Switzerland, 2013; pp. 211–230.
75. Malapermal, V.; Mbatha, J.N.; Gengan, R.M.; Anand, K. Biosynthesis of bimetallic Au-Ag nanoparticles using *Ocimum basilicum* (L.) with antidiabetic and antimicrobial properties. *Adv. Mater. Lett.* **2015**, *6*, 1050–1057. [[CrossRef](#)]
76. Nazeruddin, G.; Prasad, R.; Shaikh, Y.; Shaikh, A. Synergetic effect of Ag-Cu bimetallic nanoparticles on antimicrobial activity. *Pharm. Lett.* **2014**, *3*, 129–136.
77. Slocik, J.M.; Naik, R.R. Biologically programmed synthesis of bimetallic nanostructures. *Adv. Mater.* **2006**, *18*, 1988–1992. [[CrossRef](#)]
78. Valiyeva, G.G.; Bavasso, I.; Di Palma, L.; Hajiyeva, S.R.; Ramazanov, M.A.; Hajiyeva, F.V. Synthesis of Fe/Ni bimetallic nanoparticles and application to the catalytic removal of nitrates from water. *Nanomaterials* **2019**, *9*, 1130. [[CrossRef](#)]

79. Bensaida, K.; Eljamal, R.; Sughihara, Y.; Eljamal, O. The impact of iron bimetallic nanoparticles on bulk microbial growth in wastewater. *J. Water Process Eng.* **2020**, *40*, 101825. [[CrossRef](#)]
80. Harikumar, P.; TK, H. Application of CuNi bimetallic nanoparticle as an adsorbent for the removal of heavy metals from aqueous solution. *Int. J. Environ. Anal. Chem.* **2019**, *101*, 869–883. [[CrossRef](#)]
81. Ulucan-Altuntas, K.; Kuzu, S.L. Modelling and optimization of dye removal by Fe/Cu bimetallic nanoparticles coated with different Cu ratios. *Mater. Res. Express* **2019**, *6*, 1150a4. [[CrossRef](#)]
82. Al-Haddad, J.; Alzaabi, F.; Pal, P.; Rambabu, K.; Banat, F. Green synthesis of bimetallic copper–silver nanoparticles and their application in catalytic and antibacterial activities. *Clean Technol. Environ. Policy* **2020**, *22*, 269–277. [[CrossRef](#)]
83. Dlamini, N.G.; Basson, A.K.; Pullabhotla, V.S.R. Synthesis and Application of FeCu Bimetallic Nanoparticles in Coal Mine Wastewater Treatment. *Minerals* **2021**, *11*, 132. [[CrossRef](#)]
84. Dlamini, N.G.; Basson, A.K.; Rajasekhar Pullabhotla, V.S. Biosynthesis of biofloculant passivated copper nanoparticles, characterization and application. *Phys. Chem. Earth Parts A/B/C* **2020**, *118*, 102898. [[CrossRef](#)]
85. Zhao, Y.; Ye, C.; Liu, W.; Chen, R.; Jiang, X. Tuning the composition of AuPt bimetallic nanoparticles for antibacterial application. *Angew. Chem. Int. Ed.* **2014**, *53*, 8127–8131. [[CrossRef](#)]
86. Mazhar, T.; Shrivastava, V.; Tomar, R.S. Green synthesis of bimetallic nanoparticles and its applications: A review. *J. Pharm. Sci. Res.* **2017**, *9*, 102.
87. Moshfegh, M.; Forootanfar, H.; Zare, B.; Shahverdi, A.; Zarrini, G.; Faramarzi, M. Biological synthesis of Au, Ag and Au-Ag bimetallic nanoparticles by  $\alpha$ -amylase. *Dig. J. Nanomater. Bios.* **2011**, *6*, 1419–1426.
88. Arora, N.; Thangavelu, K.; Karanikolos, G.N. Bimetallic nanoparticles for antimicrobial applications. *Front. Chem.* **2020**, *8*, 412. [[CrossRef](#)]
89. Scaria, J.; Nidheesh, P.; Kumar, M.S. Synthesis and applications of various bimetallic nanomaterials in water and wastewater treatment. *J. Environ. Manag.* **2020**, *259*, 110011. [[CrossRef](#)]
90. Guzmán, M.G.; Dille, J.; Godet, S. Synthesis of silver nanoparticles by chemical reduction method and their antibacterial activity. *Int. J. Chem. Biomol. Eng.* **2009**, *2*, 104–111.
91. Jamkhande, P.G.; Ghule, N.W.; Bamer, A.H.; Kalaskar, M.G. Metal nanoparticles synthesis: An overview on methods of preparation, advantages and disadvantages, and applications. *J. Drug Deliv. Sci. Technol.* **2019**, *53*, 101174. [[CrossRef](#)]
92. Pantidos, N.; Horsfall, L.E. Biological synthesis of metallic nanoparticles by bacteria, fungi and plants. *J. Nanomed. Nanotechnol.* **2014**, *5*, 1. [[CrossRef](#)]
93. He, S.; Guo, Z.; Zhang, Y.; Zhang, S.; Wang, J.; Gu, N. Biosynthesis of gold nanoparticles using the bacteria *Rhodopseudomonas capsulata*. *Mater. Lett.* **2007**, *61*, 3984–3987. [[CrossRef](#)]
94. Kuppusamy, P.; Yusoff, M.M.; Maniam, G.P.; Govindan, N. Biosynthesis of metallic nanoparticles using plant derivatives and their new avenues in pharmacological applications—An updated report. *Saudi Pharm. J.* **2016**, *24*, 473–484. [[CrossRef](#)] [[PubMed](#)]
95. Bahrulolum, H.; Nooraei, S.; Javanshir, N.; Tarrahimofrad, H.; Mirbagheri, V.S.; Easton, A.J.; Ahmadian, G. Green synthesis of metal nanoparticles using microorganisms and their application in the agrifood sector. *J. Nanobiotechnol.* **2021**, *19*, 1–26. [[CrossRef](#)] [[PubMed](#)]
96. Sagadevan, S.; Imteyaz, S.; Murugan, B.; Lett, J.A.; Sridewi, N.; Weldegebriael, G.K.; Fatimah, I.; Oh, W.-C. A comprehensive review on green synthesis of titanium dioxide nanoparticles and their diverse biomedical applications. *Green Process. Synth.* **2022**, *11*, 44–63. [[CrossRef](#)]
97. Singh, A.; Gautam, P.K.; Verma, A.; Singh, V.; Shivapriya, P.M.; Shivalkar, S.; Sahoo, A.K.; Samanta, S.K. Green synthesis of metallic nanoparticles as effective alternatives to treat antibiotics resistant bacterial infections: A review. *Biotechnol. Rep.* **2020**, *25*, e00427. [[CrossRef](#)] [[PubMed](#)]
98. Sathiyarayanan, G.; Kiran, G.S.; Selvin, J. Synthesis of silver nanoparticles by polysaccharide biofloculant produced from marine *Bacillus subtilis* MSBN17. *Colloids Surf. B Biointerfaces* **2013**, *102*, 13–20. [[CrossRef](#)]
99. Khanna, P.; Gaikwad, S.; Adhyapak, P.; Singh, N.; Marimuthu, R. Synthesis and characterization of copper nanoparticles. *Mater. Lett.* **2007**, *61*, 4711–4714. [[CrossRef](#)]
100. Sun, Y.-P.; Li, X.-Q.; Cao, J.; Zhang, W.-X.; Wang, H.P. Characterization of zero-valent iron nanoparticles. *Adv. Colloid Interface Sci.* **2006**, *120*, 47–56. [[CrossRef](#)]
101. Shao, F.; Zhou, S.; Xu, J.; Du, Q.; Chen, J.; Shang, J. Detoxification of Cr (VI) using biochar-supported Cu/Fe bimetallic nanoparticles. *Desalin. Water Treat* **2019**, *158*, 121–129. [[CrossRef](#)]
102. Shi, S.; Han, X.; Liu, J.; Lan, X.; Feng, J.; Li, Y.; Zhang, W.; Wang, J. Photothermal-boosted effect of binary CuFe bimetallic magnetic MOF heterojunction for high-performance photo-Fenton degradation of organic pollutants. *Sci. Total Environ.* **2021**, *795*, 148883. [[CrossRef](#)]
103. Younas, U.; Hassan, S.T.; Ali, F.; Hassan, F.; Saeed, Z.; Pervaiz, M.; Khan, S.; Jannat, F.T.; Bibi, S.; Sadiqa, A. Radical scavenging and catalytic activity of Fe-Cu bimetallic nanoparticles synthesized from *Ixora finlaysoniana* extract. *Coatings* **2021**, *11*, 813. [[CrossRef](#)]
104. Rasool, U.; Hemalatha, S. Marine endophytic actinomycetes assisted synthesis of copper nanoparticles (CuNPs): Characterization and antibacterial efficacy against human pathogens. *Mater. Lett.* **2017**, *194*, 176–180. [[CrossRef](#)]
105. Mata, Y.; Torres, E.; Blazquez, M.; Ballester, A.; González, F.; Muñoz, J. Gold (III) biosorption and bioreduction with the brown alga *Fucus vesiculosus*. *J. Hazard. Mater.* **2009**, *166*, 612–618. [[CrossRef](#)]

106. Wang, J.; Liu, C.; Hussain, I.; Li, C.; Li, J.; Sun, X.; Shen, J.; Han, W.; Wang, L. Iron–copper bimetallic nanoparticles supported on hollow mesoporous silica spheres: The effect of Fe/Cu ratio on heterogeneous Fenton degradation of a dye. *RSC Adv.* **2016**, *6*, 54623–54635. [[CrossRef](#)]
107. Stefaniuk, M.; Oleszczuk, P.; Ok, Y.S. Review on nano zerovalent iron (nZVI): From synthesis to environmental applications. *Chem. Eng. J.* **2016**, *287*, 618–632. [[CrossRef](#)]
108. Dlamini, N.G.; Basson, A.K.; Pullabhotla, R.V. Wastewater treatment by a polymeric biofloculant and iron nanoparticles synthesized from a biofloculant. *Polymers* **2020**, *12*, 1618. [[CrossRef](#)]
109. Velidandi, A.; Sarvepalli, M.; Pabbathi, N.P.P.; Baadhe, R.R. Biogenic synthesis of novel platinum-palladium bimetallic nanoparticles from aqueous *Annona muricata* leaf extract for catalytic activity. *3 Biotech* **2021**, *11*, 385. [[CrossRef](#)]
110. Akilandaeaswari, B.; Muthu, K. One-pot green synthesis of Au–Ag bimetallic nanoparticles from *Lawsonia inermis* seed extract and its catalytic reduction of environmental polluted methyl orange and 4-nitrophenol. *J. Taiwan Inst. Chem. Eng.* **2021**, *127*, 292–301. [[CrossRef](#)]
111. Botha, T.L.; Elemike, E.E.; Horn, S.; Onwudiwe, D.C.; Giesy, J.P.; Wepener, V. Cytotoxicity of Ag, Au and Ag–Au bimetallic nanoparticles prepared using golden rod (*Solidago canadensis*) plant extract. *Sci. Rep.* **2019**, *9*, 4169. [[CrossRef](#)]
112. Dsouza, A.; Shilpa, M.; Gurumurthy, S.; Nagaraja, B.; Mundinamani, S.; Ramam, K.; Gedda, M.; Murari, M. CuAg and AuAg bimetallic nanoparticles for catalytic and heat transfer applications. *Clean Technol. Environ. Policy* **2021**, *23*, 2145–2155. [[CrossRef](#)]
113. Wang, H.; Zhou, W.; Liu, J.-X.; Si, R.; Sun, G.; Zhong, M.-Q.; Su, H.-Y.; Zhao, H.-B.; Rodriguez, J.A.; Pennycook, S.J. Platinum-modulated cobalt nanocatalysts for low-temperature aqueous-phase Fischer–Tropsch synthesis. *J. Am. Chem. Soc.* **2013**, *135*, 4149–4158. [[CrossRef](#)] [[PubMed](#)]
114. Akinsiku, A.A.; Dare, E.O.; Ajani, O.O.; Ayo-Ajayi, J.; Ademosun, O.T.; Ajayi, S.O. Room temperature Phytosynthesis of Ag/Co bimetallic nanoparticles using aqueous leaf extract of *Canna indica*. In *IOP Conference Series: Earth and Environmental Science*; IOP Publishing: Bristol, UK, 2018; p. 012019.
115. Roopan, S.M.; Surendra, T.V.; Elango, G.; Kumar, S.H.S. Biosynthetic trends and future aspects of bimetallic nanoparticles and its medicinal applications. *Appl. Microbiol. Biotechnol.* **2014**, *98*, 5289–5300. [[CrossRef](#)] [[PubMed](#)]
116. McClements, D.J.; Öztürk, B. Utilization of nanotechnology to improve the application and bioavailability of phytochemicals derived from waste streams. *J. Agric. Food Chem.* **2021**, *70*, 6884–6900. [[CrossRef](#)]
117. Khodamorady, M.; Sohrabnezhad, S.; Bahrami, K. Efficient one-pot synthetic methods for the preparation of 3, 4-dihydropyrimidinones and 1, 4-dihydropyridine derivatives using BNPs@ SiO<sub>2</sub> (CH<sub>2</sub>)<sub>3</sub>NHSO<sub>3</sub>H as a ligand and metal free acidic heterogeneous nano-catalyst. *Polyhedron* **2020**, *178*, 114340. [[CrossRef](#)]
118. Minal, S.P.; Prakash, S. Laboratory analysis of Au–Pd bimetallic nanoparticles synthesized with *Citrus limon* leaf extract and its efficacy on mosquito larvae and non-target organisms. *Sci. Rep.* **2020**, *10*, 21610. [[CrossRef](#)]
119. Manickam-Periyaraman, P.; Espinosa, J.C.; Ferrer, B.; Subramanian, S.; Álvaro, M.; García, H.; Navalón, S. Bimetallic iron-copper oxide nanoparticles supported on nanometric diamond as efficient and stable sunlight-assisted Fenton photocatalyst. *Chem. Eng. J.* **2020**, *393*, 124770. [[CrossRef](#)]
120. de França Bettencourt, G.M.; Degenhardt, J.; Torres, L.A.Z.; de Andrade Tanobe, V.O.; Soccol, C.R. Green biosynthesis of single and bimetallic nanoparticles of iron and manganese using bacterial auxin complex to act as plant bio-fertilizer. *Biocatal. Agric. Biotechnol.* **2020**, *30*, 101822. [[CrossRef](#)]
121. Zin, M.T.; Borja, J.; Hinode, H.; Kurniawan, W. Synthesis of bimetallic Fe/Cu nanoparticles with different copper loading ratios. *Dimensions* **2013**, *13*, 1031–1035.
122. Fang, L.; Xu, C.; Zhang, W.; Huang, L.-Z. The important role of polyvinylpyrrolidone and Cu on enhancing dechlorination of 2,4-dichlorophenol by Cu/Fe nanoparticles: Performance and mechanism study. *Appl. Surf. Sci.* **2018**, *435*, 55–64. [[CrossRef](#)]
123. Ngema, S.; Basson, A.; Maliehe, T. Synthesis, characterization and application of polyacrylamide grafted biofloculant. *Phys. Chem. Earth Parts A/B/C* **2020**, *115*, 102821. [[CrossRef](#)]
124. Beyth, N.; Hourri-Haddad, Y.; Domb, A.; Khan, W.; Hazan, R. Alternative antimicrobial approach: Nano-antimicrobial materials. *Evid. Based Complement. Altern. Med.* **2015**, *2015*, 246012. [[CrossRef](#)]
125. Tao, F.F. Synthesis, catalysis, surface chemistry and structure of bimetallic nanocatalysts. *Chem. Soc. Rev.* **2012**, *41*, 7977–7979. [[CrossRef](#)] [[PubMed](#)]
126. Turakhia, B.; Turakhia, P.; Shah, S. Green synthesis of zero valent iron nanoparticles from *Spinacia oleracea* (spinach) and its application in waste water treatment. *J. Adv. Res. Appl. Sci* **2018**, *5*, 46–51.
127. Schindler, D.W. Evolution of phosphorus limitation in lakes: Natural mechanisms compensate for deficiencies of nitrogen and carbon in eutrophied lakes. *Science* **1977**, *195*, 260–262. [[CrossRef](#)]
128. Bennett, E.M.; Carpenter, S.R.; Caraco, N.F. Human impact on erodable phosphorus and eutrophication: A global perspective: Increasing accumulation of phosphorus in soil threatens rivers, lakes, and coastal oceans with eutrophication. *BioScience* **2001**, *51*, 227–234. [[CrossRef](#)]
129. Bhatnagar, A.; Sillanpää, M. A review of emerging adsorbents for nitrate removal from water. *Chem. Eng. J.* **2011**, *168*, 493–504. [[CrossRef](#)]
130. Liu, Y.; Majetich, S.A.; Tilton, R.D.; Sholl, D.S.; Lowry, G.V. TCE dechlorination rates, pathways, and efficiency of nanoscale iron particles with different properties. *Environ. Sci. Technol.* **2005**, *39*, 1338–1345. [[CrossRef](#)]
131. Rao, E.P.; Puttanna, K. Nitrates, agriculture and environment. *Curr. Sci.* **2000**, *79*, 1163–1168.

132. Majumdar, D.; Gupta, N. Nitrate pollution of groundwater and associated human health disorders. *Indian J. Environ. Health* **2000**, *42*, 28–39.
133. Forde, B.G. Nitrate transporters in plants: Structure, function and regulation. *Biochim. Biophys. Acta Biomembr.* **2000**, *1465*, 219–235. [[CrossRef](#)]
134. Fewtrell, L. Drinking-water nitrate, methemoglobinemia, and global burden of disease: A discussion. *Environ. Health Perspect.* **2004**, *112*, 1371–1374. [[CrossRef](#)]
135. Sparis, D.; Mystrioti, C.; Xenidis, A.; Papassiopi, N. Reduction of nitrate by copper-coated ZVI nanoparticles. *Desalination Water Treat.* **2013**, *51*, 2926–2933. [[CrossRef](#)]
136. Albert, M.J.; Faruque, A.; Faruque, S.; Sack, R.; Mahalanabis, D. Case-control study of enteropathogens associated with childhood diarrhea in Dhaka, Bangladesh. *J. Clin. Microbiol.* **1999**, *37*, 3458–3464. [[CrossRef](#)]
137. Wang, J.; Chen, C. Biosorbents for heavy metals removal and their future. *Biotechnol. Adv.* **2009**, *27*, 195–226. [[CrossRef](#)]
138. Faisal, M.; Khan, S.B.; Rahman, M.M.; Jamal, A.; Akhtar, K.; Abdullah, M. Role of ZnO-CeO<sub>2</sub> nanostructures as a photo-catalyst and chemi-sensor. *J. Mater. Sci. Technol.* **2011**, *27*, 594–600. [[CrossRef](#)]
139. Khan, S.B.; Faisal, M.; Rahman, M.M.; Jamal, A. Exploration of CeO<sub>2</sub> nanoparticles as a chemi-sensor and photo-catalyst for environmental applications. *Sci. Total Environ.* **2011**, *409*, 2987–2992. [[CrossRef](#)]
140. Padhi, B. Pollution due to synthetic dyes toxicity & carcinogenicity studies and remediation. *Int. J. Environ. Sci.* **2012**, *3*, 940–955.
141. Wang, C.; Yediler, A.; Lienert, D.; Wang, Z.; Kettrup, A. Toxicity evaluation of reactive dyestuffs, auxiliaries and selected effluents in textile finishing industry to luminescent bacteria *Vibrio fischeri*. *Chemosphere* **2002**, *46*, 339–344. [[CrossRef](#)]
142. El Gaini, L.; Lakraimi, M.; Sebbar, E.; Meghea, A.; Bakasse, M. Removal of indigo carmine dye from water to Mg–Al–CO<sub>3</sub>-calcined layered double hydroxides. *J. Hazard. Mater.* **2009**, *161*, 627–632. [[CrossRef](#)]
143. Bedoui, A.; Ahmadi, M.; Bensalah, N.; Gadri, A. Comparative study of Eriochrome black T treatment by BDD-anodic oxidation and Fenton process. *Chem. Eng. J.* **2009**, *146*, 98–104. [[CrossRef](#)]
144. Ayed, L.; Mahdhi, A.; Cheref, A.; Bakhrouf, A. Decolorization and degradation of azo dye Methyl Red by an isolated *Sphingomonas paucimobilis*: Biototoxicity and metabolites characterization. *Desalination* **2011**, *274*, 272–277. [[CrossRef](#)]
145. Gul, S.; Rehan, Z.A.; Khan, S.A.; Akhtar, K.; Khan, M.A.; Khan, M.; Rashid, M.I.; Asiri, A.M.; Khan, S.B. Antibacterial PES-CA-Ag<sub>2</sub>O nanocomposite supported Cu nanoparticles membrane toward ultrafiltration, BSA rejection and reduction of nitrophenol. *J. Mol. Liq.* **2017**, *230*, 616–624. [[CrossRef](#)]
146. Haider, S.; Kamal, T.; Khan, S.B.; Omer, M.; Haider, A.; Khan, F.U.; Asiri, A.M. Natural polymers supported copper nanoparticles for pollutants degradation. *Appl. Surf. Sci.* **2016**, *387*, 1154–1161. [[CrossRef](#)]
147. Lindholm-Lehto, P.C.; Knuutinen, J.S.; Ahkola, H.S.; Herve, S.H. Refractory organic pollutants and toxicity in pulp and paper mill wastewaters. *Environ. Sci. Pollut. Res.* **2015**, *22*, 6473–6499. [[CrossRef](#)]
148. Ismail, M.; Khan, M.; Khan, S.B.; Khan, M.A.; Akhtar, K.; Asiri, A.M. Green synthesis of plant supported CuAg and CuNi bimetallic nanoparticles in the reduction of nitrophenols and organic dyes for water treatment. *J. Mol. Liq.* **2018**, *260*, 78–91. [[CrossRef](#)]

**Disclaimer/Publisher’s Note:** The statements, opinions and data contained in all publications are solely those of the individual author(s) and contributor(s) and not of MDPI and/or the editor(s). MDPI and/or the editor(s) disclaim responsibility for any injury to people or property resulting from any ideas, methods, instructions or products referred to in the content.